Assessing the impact of sewage overflows on oyster harvest areas: Technical Summary Report

WRL TR 2023/32, May 2025

By A J Harrison, M Mason, Y Doherty and B M Miller

UNSW
Water Research
Laboratory

UNSW
SYDNEY

UNSW
Water Research
Laboratory

UNSW
SYDNEY

Assessing the impact of sewage overflows on oyster harvest areas: Technical Summary Report

WRL TR 2023/32, May 2025

By A J Harrison, M Mason, Y Doherty and B M Miller

Project details

Report title	Assessing the impact of sewage overflows on oyster harvest areas: Technical Summary Report
Authors(s)	A J Harrison, M Mason, Y Doherty and B M Miller
Report no.	2023/32
Report status	Final
Date of issue	May 2025
WRL project no.	2021101
Project manager	A J Harrison
Client	Department of Regional NSW
Funding acknowledgement	This study was funded through a Department of Regional NSW Storm And Flood Industry Recovery Program (SFIRP) – Sector Recovery and Resilience Grant with support from local councils and wastewater authorities

Document status

Version	Reviewed by	Approved by	Date issued
Preliminary draft	BMM	IRC	21/01/25
Final	BMM	FF	26/05/25

This report should be cited as: Harrison, AJ, Mason, M, Doherty, Y and Miller, BM 2025, Assessing the impact of sewage overflows on oyster harvest areas: Technical Summary Report, WRL Technical Report 2023/32, UNSW Water Research Laboratory.

UNSW
Water Research
Laboratory

www.wrl.unsw.edu.au
110 King St Manly Vale NSW 2093 Australia
Tel +61 (2) 8071 9800 ABN 57 195 873 179

This project has been funded under the Storm and Flood Industry Recovery program, jointly funded by the Australian and NSW governments. Although funding for this project has been provided by both Australian and NSW governments, the material contained herein does not necessarily represent the views of either government.

Contents

List of tables

List of figures

1 Introduction

1.1 Project overview

The Water Research Laboratory (WRL) of the School of Civil and Environmental Engineering at UNSW Sydney was engaged to undertake a large study titled “Assessing the impact of sewage overflows on oyster harvest areas in NSW”. This study was funded through a Department of Regional NSW Storm and Flood Industry Recovery Program (SFIRP) – Sector Recovery and Resilience grant with support from local councils and wastewater authorities.

The study seeks to understand the fate of contaminants and the potential exposure of oyster leases following overflow events under different environmental conditions including tides, wind, and catchment runoff. The results of this study provide decision makers with quantitative data to assess exposure risk to specific harvest areas on an individual sewer overflow event basis. These outcomes allow for increased confidence in ensuring consumer safety, and more targeted harvest area closures to reduce the economic impact of widespread closures on local industry.

Sewage overflows into estuaries occur under a range of conditions, often due to malfunctioning or overwhelmed infrastructure. As a result, the environmental conditions in the estuary at the time of an overflow can vary. While experimental data such as large scale dye release experiments can be useful to understand contaminant transport in a single set of conditions (or a small number of conditions), it is impractical to collect such data for the broad range of conditions possible across multiple sewage overflow locations. Therefore, the approach of this study (Figure 1-1) is to combine numerical modelling and site-specific field investigations as a cost-effective means to gain sufficient understanding of contaminant transport.

1.2 Report context

This report provides a technical summary of the methods of data collation, fieldwork data collection and numerical modelling utilised for all estuaries in this study and is intended to be used by technical experts to understand and replicate the study outcomes. A summary of the study findings for decision-makers is provided in WRL TR2024/26. It also includes an overview on how to interpret and use the results from this study for understanding risks following future overflow events.

This report is supported by individual technical reports for each estuary included in the study, which are also intended for technical experts. A summary of all reports published for this study is provided below in Table 1-1 and Table 1-2.

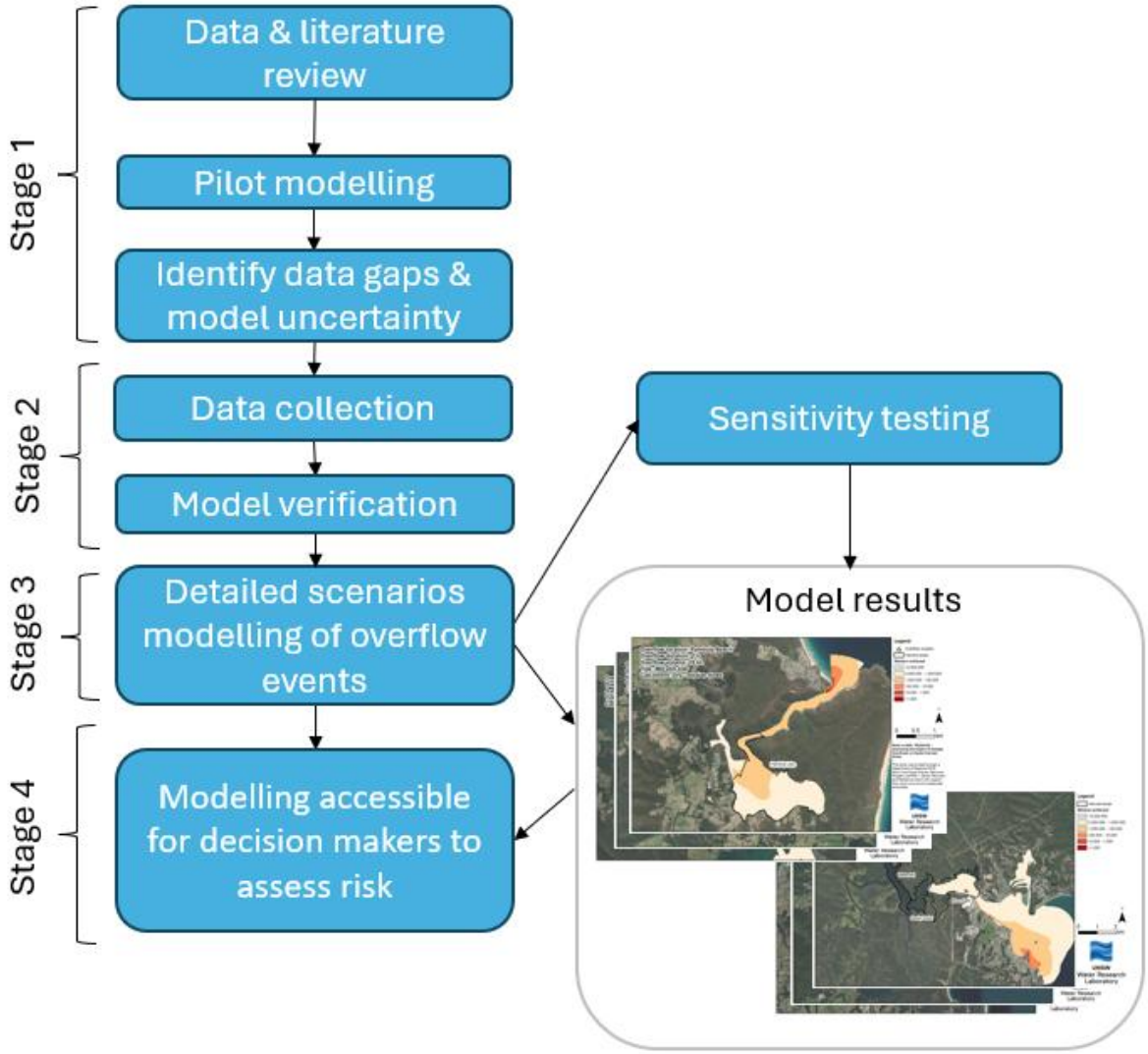

Figure 1-1 Project overview

Table 1-1 Summary of project reference documents

Report Number	Intention
WRL TR2024/26	Project overview and user guide
WRL TR2023/32 (this report)	Summary of technical methods

Table 1-2 Summary of estuary specific reports

Estuary	Technical summary
Tweed River	WRL TR2023/18
Nambucca River	WRL TR2023/19
Hastings River	WRL TR2025/05
Camden Haven River	WRL TR2023/20
Wallis Lake	WRL TR2023/21
Port Stephens	WRL TR2023/22
Clyde River	WRL TR2023/24
Shoalhaven/Crookhaven Rivers	WRL TR2023/23
Wagonga Inlet	WRL TR2023/25
Merimbula Lake	WRL TR2023/26
Pambula Lake	WRL TR2023/27

1.3 About this report

This report includes the following sections:

- **Section 2: Existing data collation** – summarises key datasets that were utilised
- **Section 3: Pilot modelling and data gaps** – outlines the function and construction of pilot models
- **Section 4: Field data collection** – summarises the field data collection techniques
- **Section 5: Numerical modelling package** – summarises the RMA modelling packages used in this study
- **Section 6: Hydrodynamic model development** – summarises the construction of the hydrodynamic numerical model
- **Section 7: Water quality model development** – summarises the construction of the water quality numerical model
- **Section 8: Scenario modelling** – describes the considerations for the scenario modelling across each of the estuaries

2 Existing data collation

2.1 Preamble

Many of the estuaries in NSW have had substantial field data collection campaigns in the past which are relevant to the development of hydrodynamic and water quality models. Where possible, this data has been reviewed for this study, and utilised where possible to maximise the capacity of the models. This section includes a brief description of key datasets, as well as some of the larger resources that have coverage across much of the state. Details of site specific datasets are also provided in the technical data and modelling report for each estuary (refer Table 1-2).

2.2 Bathymetry

Bathymetry data is vital to developing numerical models of estuarine systems as it influences flow paths, frictional losses and tidal volumes. Table 2-1 summarises the key bathymetric datasets used across all estuaries. Preference for bathymetric data was typically given to the most recent data sources, particularly in areas which experience significant bathymetric changes through time. In some cases, specific local data was available in addition to those tabulated below, however this is discussed in the estuary specific reports. Key features and uncertainties are also discussed in the individual reports.

Table 2-1 Key bathymetric existing data sources

Source	Date of collection	Comment
NSW Marine LiDAR (DPIE, 2018)	2018	Limited coverage within estuaries (typically only covering 0.5 – 1 km near the coast), however is typically the most recent dataset.
Single and multi-beam bathymetric surveys (OEH, 2022a; OEH, 2022b)	1970s – 2023, depending on location	Good coverage of most NSW estuaries, although dated in some locations.
Australian Hydrographic Office Navigational charts (AHO, 2024a; AHO, 2024b)	Varied	Good coverage of all estuaries, however the data is typically quite old.
Crowd sourced boat sonar mapping (NAVONICS, 2023)	Continuous data collection	No quality assurance available. This data was used to approximate areas to a higher resolution where limited other data was also available.
High resolution aerial imagery (NearMap, 2024)	2014 – 2023	Imagery used to assess movement of readily visible shallow bars and channels where bathymetry is known to regularly change.

2.3 Water level and flow gauging

Understanding the hydrodynamic behaviour of an estuary is important to modelling pollutant transport. Collection of hydrodynamic data relevant for numerical model development typically includes measurements of water levels, water velocity and flow. Measurements of tidal flow and tidal velocity are essential for good calibration of a hydrodynamic model. Without this data, it is difficult to assess the accuracy of the model at replicating the tidal prism of an estuary (i.e., how much water goes in and out on every tide).

Manly Hydraulics Laboratory (MHL) has been collecting substantial hydrodynamic data in each of the study areas since the 1970's through to the present. Datasets include both water level and tidal flow data (see Table 2-2). Notably, in the late 1990's and early 2000's as part of the NSW Department of Land and Water Conservation's Estuary Management Program, intensive field data campaigns were undertaken. These studies collected tidal flow gauging over a full tidal cycle for most of the study estuaries. This data was provided by MHL for use in model validation for this project.

In addition to intensive flow data collection, MHL also maintain a substantial network of water level loggers that record levels (referenced to Australian Height Datum) across estuaries in NSW. There are typically between one and five loggers available in each estuary, and data from each relevant logger has been provided for this study.

Table 2-2 Manly Hydraulics Laboratory - key hydrodynamic data

Data program	Temporal nature	Period of acquisition	Data available
Tidal data collection studies	Intensive 1 - 5 day data collection campaign	Varied, typically late 1990's to early 2000's	Tidal flow/velocity gauging at key locations Short term water level data
Long term water level data	Continuous (every 15 minutes)	Varied, typically from the late 1990's to present	Long term water level data

2.4 Catchment inflows

Continuous flow gauging of discharge and water level data is available for most major rivers in NSW on the WaterNSW portal (WaterNSW, 2023). Flow gauging data is typically derived from a telemetered water level logger with an associated flow rating curve. For the estuaries included in this study, all flow gauging in the relevant catchments was downloaded from the WaterNSW portal.

The models being developed for this project extend to the tidal limit of each estuary. Catchment runoff (streamflow) from upstream of the tidal limit are applied to the model as upstream inflow boundary conditions. As the flow gauging stations generally do not coincide with the tidal limit, a scaling parameter was applied to the WaterNSW gauged flows to incorporate catchment areas between the gauge and the tidal limit. This was done by computing the ratio of the total catchment area upstream of the tidal limit to the catchment area upstream of the gauge. The gauged catchment streamflow was then multiplied by this ratio (scale factor) to obtain the streamflow applied at the model boundary. For example, if a gauged catchment was half the size of the catchment upstream of the model boundary,

the scale factor would be two, and the observed flow at the gauge multiplied by two would be entered into the model. Catchments were delineated using digital elevation models accessed from the Geoscience Australia's 1 second digital elevation models by Gallant et al. (2011) and standard GIS techniques. When a model upstream catchment did not contain a flow gauge, an appropriate nearby gauged catchment was used, with the assumption that rainfall and runoff characteristics would be similar.

This approach (weighted gauged catchments) was used rather than defining rainfall runoff relationships, as most estuaries had long term streamflow data which covered the majority of the area of the model inflow catchments. For some estuaries, flow gauging data was not available for all model inflow catchments. In these cases, a nearby gauged catchment was assessed to ensure it was likely to be representative of the model inflow catchment. This creates increased uncertainty, however for estuaries with less through streamflow data (such as Wagonga, Merimbula and Wallis), catchments tended to be small relative to estuary area and hence upstream inflows are less important. Thus, weighted gauged catchments were deemed appropriate for this study, although a different approach may be needed if the model is used for a different application.

2.5 Sewage overflow data

Centralised wastewater treatment systems are typically managed by the local council or other legislated wastewater authority (such as Hunter Water Corporation). These systems generally include a reticulation network of pipes and sewage pumping stations (SPS) which connect to local wastewater treatment plants (WWTP). Overflows from the reticulation network and WWTPs occur during both dry and wet weather. This can result in partially or fully untreated effluent being discharged into adjacent waterways. In some locations, privately owned and managed septic systems may also result in sewage overflows. Overflows into estuarine systems may result in high virus and bacterial loads which can then be transported to oyster harvest areas by advection and dispersion. As bivalve filter feeders, effluent can be ingested and retained by oysters which then pose a human health risk when consumed. When overflows occur and no mitigation measures are in place to prevent effluent from reaching estuarine systems, the local sewage management authority is required to notify NSW Food Authority, who will decide whether harvest area closures are necessary.

Dry weather overflows typically occur from the reticulation network due to a blockage or pump failure (e.g. electrical fault). To prevent sewage backing up in the reticulation network, wastewater is diverted under gravity through designated overflow locations (refer Figure 2-1). Dry weather overflows often occur at a relatively low flow rate and for a short duration, typically hours. As there is no treatment or dilution, the overflow is comprised of raw sewage with potentially high bacterial/pathogen concentrations. Sewage overflows during dry weather generally coincide with limited catchment runoff and low waterway flows. Dry weather overflows do not typically occur from WWTPs due to the adequate storage capacity of the WWTP. Information relating to dry weather overflows is often limited to location only, with volume and duration typically estimated based on the time of reporting and the time of the fault rectification. Notifications are often made by the public or utility employees and may not coincide with the onset of sewage spilling, which leads to further uncertainty in the risk.

Figure 2-1 Example of a sewage pumping station overflow point (Careel Bay, Pittwater)

Wet weather overflows can occur from both the reticulation network and WWTPs. These events are generally caused by the capacity of the system being overwhelmed by stormwater ingress, or the inundation of a SPS during flooding. Wet weather overflows can occur for an extended duration (hours to days) with a varying volume and pathogen concentration. Wet weather overflows tend to coincide with periods of high catchment runoff or river inflows, which increases the mobility of the plume and also leads to greater levels of dilution. Data relating to wet weather overflows from the network or SPS is also limited. Data relating to WWTP wet weather overflows includes additional information as flow rates (volume) and duration are often more easily quantified through the infrastructure at these sites.

Sewage overflows reported to NSW Food Authority since 2016 were provided for consideration in this study. Typically, the locations of the sewage overflows are well understood and reported by local wastewater authorities. The volume and duration of overflows is less documented, however, this has been provided where possible. The location of historical overflows has been used to determine the locations of overflows being modelled in each estuary.

2.6 Existing models

In some cases, existing models were available from previous studies in some of the estuaries. Where possible, data from existing models were used in this study. This included consideration of:

- Model mesh and geometry
- Bathymetry
- Model boundaries
- Model friction parameters

Typically, substantial changes were required in the redevelopment of the models as prior models were not created for water quality modelling. Details of existing models (where relevant) is provided in each of the estuary specific reports (refer Table 1-2).

3 Pilot modelling and data gaps

3.1 Preamble

Pilot modelling refers to the rapid development of preliminary numerical models based on the available information. While pilot model test results are not typically suitable for decision making, pilot modelling was an integral part of Stage 1 of the project to highlight key sources of uncertainty that would impact the final modelling.

While the details of the model development are discussed in detail in Section 5 (Numerical model packages), Section 6 (Hydrodynamic model development) and Section 7 (Water quality model development), this section provides a brief description of the development and purpose of the pilot modelling in this project.

3.2 Pilot model development

Following the collation of existing models and data for each of the study locations, a pilot model was developed for each estuary. Pilot model mesh development was based on available bathymetric data, aerial imagery, and existing models. The models covered the tidal extent of each estuary, which ensures that the tidal prism is represented in the model. The pilot models developed include coupled hydrodynamic and water quality components.

Boundary conditions, including tidal water levels and catchment inflows, were included in the hydrodynamic model, allowing the model to be run to replicate a certain period of time. As high-quality tidal flow data was available through the MHL data collection campaigns (Section 6.4), models were typically set up to run these periods to test the model's capacity to replicate flows throughout the system. Internal model parameters (such as friction and turbulence) were adjusted within reasonable limits to test the model's initial capacity to replicate hydrodynamic behaviour prior to the field data campaigns. This allowed for the identification of areas where data gaps remained that could impact the model's capacity to be used for decision-making.

3.3 Data gaps

Pilot modelling was an integral part of Stage 1 of the project to highlight key sources of uncertainty that would impact the final modelling. Pilot modelling generally highlighted key data that could then be collected in the targeted field campaigns to reduce uncertainty. From the hydrodynamic modelling, this typically included:

- Identify gaps in the existing data, including gaps in bathymetry or flow data
- Understand important hydrodynamic features, including mobile shoals, submerged breakwaters or high velocity channels
- Locating areas which were poorly calibrated to observe flows and were important to advection and dispersion around the oyster harvest areas
- Understand tidal time lags and water level attenuation/dampening

Two main processes move constituents within water bodies: advection which is movement with the current; and dispersion which is mixing, which causes the constituent to spread and disperse.

For most estuaries, the existing data to validate the advection (currents) in the models was typically good. Some additional hydrodynamic data was needed to test the models' ability to predict flow and currents in another period (as further validation) and some specific flow measurements were required in particular areas of interest.

However, little to no data was available to calibrate or validate the rates of dispersion. Salinity data can be used to validate rates of dispersion in numerical water quality models, however, density differences influence mixing, particularly during the re-intrusion of salinity into an estuary following a fresh event. However, this approach was deemed inappropriate for this project, as the impact of sewer overflows on oyster leases typically have the greatest impact in the first tidal cycle to a day following the event, in the early stages of plume dilution. Targeted data collection to validate the dispersion coefficients was deemed essential and was targeted throughout the field data campaign across all estuaries.

4 Field data collection

4.1 Preamble

While a substantial amount of data was available for model development, the data gaps discussed in Section 3.3 required additional field data collection. This section summarises the methods used for field data collection.

4.2 Tidal flow gauging

Tidal flow gauging was completed in strategic locations in each estuary. Flow was either measured using a boat-mounted Sontek RiverSurveyor M9 ADCP (Acoustic Doppler Current Profiler) or a 600kHz RDI Workhorse II ADCP, as shown in Figure 4-1. These instruments use acoustic frequencies to determine velocity throughout the water column, as well as a conventional echosounder to measure depth. By driving the boat across a cross section of a river, the velocity can be integrated across the channel to estimate total discharge at a given location and time. In tidal reaches of estuaries, taking multiple measurements of discharge over the tidal cycle provides information on the dynamic changes in flow over different tides and the total tidal prism.

Figure 4-1 Boat mounted Sontek M9 ADCP (in water) and RTK GPS (top)

The advantage of the boat mounted acoustic doppler system, rather than longer term deployment of an ADCP at a single location on the bed of a channel, is that it provides a more accurate measurement of total discharge by accounting for differences in velocity across a channel. In complex systems, such as sinuous estuarine channels with complex bathymetry and high flow, this can reduce the margin of error in the measurements significantly. Being boat mounted also allows for measurements to be taken at multiple locations throughout the estuary. However, as it is not a continuously deployed instrument, the timing of measurements must be carefully planned to ensure data is collected at the stages of the tide of most importance.

For this study, flow data was not intended to capture the full stage tidal gauging, which typically requires a vessel repeatedly recording flow over a 12+ hour period. For all the estuaries in this study, full stage tidal gauging was available from the MHL intensive field data collection (Section 2.3). Rather, data was captured at multiple locations with the vessel moving about the estuary. Key stages of the tide were typically targeted during the field campaigns for this study, including peak flood or ebb tide discharge and the timing of the change of the tide. This data was then used to verify each model's capacity to estimate maximum flow, as well as tidal lags. Similarly, this data is also used to identify parts of the channel with peak velocities, which can be compared to the model.

As ADCP's measure velocity vertically through the water column, as well as across the channel, the data is useful for understanding flow stratification where the surface velocities are different to those at the bed. Figure 4-2 shows an example of data collected on the Hastings River, showing that velocities were observed to be higher at the surface of the water column than the bed. This can happen due to density differences and/or friction effects, and is important for understanding the transport of contaminant plumes. This has been considered in the modelling to estimate travel time of the plumes, discussed further in Section 7.5.

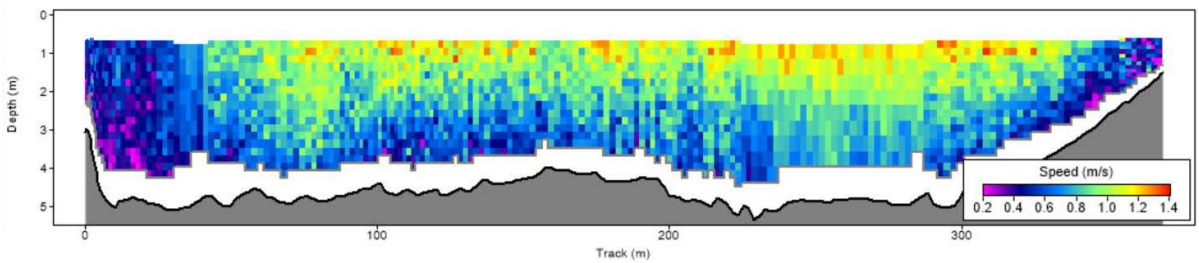

Figure 4-2 Example of measured vertical distribution of velocity on the Hastings River

4.3 Bathymetry and elevation surveys

Bathymetry in shallow estuaries is subject to change where there are sufficient water velocities and moving sediments. Large scale bathymetric surveys were not completed in this project. However, targeted and opportunistic bathymetric surveys were completed using the ADCP (see Section 4.2) combined with a Trimble RTK GPS unit. This data assisted in understanding changes in the estuaries since the last large scale bed mapping was available.

The depth of the water below the ADCP was recorded at 10 Hz, while the elevation (in metres above AHD) of the GPS unit was recorded simultaneously. With a known elevation offset between the two instruments, this data would be post-processed to get bathymetry referenced to AHD (using AusGeoid2020). In shallow intertidal areas or key structures (e.g. weirs), the RTK GPS was used without the need for an echosounder. The vertical accuracy of these surveys is estimated to be ±20 cm.

4.4 Rhodamine WT dye releases

Dye experiments provide a method to directly measure and observe dispersion in study locations under a controlled scenario. The use of dye tracers is a well-established method of conducting field measurement of dispersion from a point source or continuous discharge. Data from these field experiments was used to parameterise the water quality model, as well as to test the model's capacity to replicate the experiment.

For this project, dye experiments used Rhodamine WT. Rhodamine WT (20% active) is a non-toxic, fluorescent dye which is used to detect transport in waterways. The adopted technique was to discharge a point source of Rhodamine of a known volume (typically 500 mL) into the estuary and to then track the dye using a Turner Designs C3 fluorimeter, mounted on a boat (Figure 4-3).

Rhodamine WT is typically visible at concentrations above 5 ppb, depending on water clarity. However, readings of concentrations were monitored in real-time to allow the plume to be tracked beyond the visible range from the moving vessel. For some estuaries, a YSI Exo3 Sonde fluorimeter was also used and anchored at a fixed location of interest (e.g. a harvest area). The initial Rhodamine release concentration was 200,000,000 ppb in all instances. Both fluorimeters were calibrated to measure concentrations between 0.5 – 100 ppb. Although concentrations outside of this range were recorded by both instruments, the accuracy is reduced.

While tracking the plume, WRL staff undertook transects which crossed the plume in either the longitudinal or transverse direction with the fluorimeter at approximately 0.5 m below the surface. Primarily transects aimed to intersect the peak of the plume. However, in some cases multiple transects were done at the same location to record the passage of the plume past that location. To understand mixing over depth, the C3 fluorimeter was lowered through the water column periodically to observe the vertical mixing of the plume. A detailed description of how this data was used to estimate dispersion is provided in Section 7.2 and 7.3.

Figure 4-3 Setup with C3 Fluorimeter used for tracing Rhodamine WT

4.5 GPS drifter drogue releases

GPS drifter drogues are instruments consisting of a surface float with GPS tracking, attached to a weighted drag net set to the depth where currents are to be monitored (approximately 1 m) as shown in Figure 4-4. During the field campaign, the drogues were released at strategic locations in each estuary to assist in understanding potential advection of plumes within the estuary. A typical drogue release would involve the release of three or four drogues across the width of the channel. The drogues are then tracked using the internal GPS logger as they move autonomously with the current for periods of up to 6 hours.

Due to the submerged drag net, drogues regularly get caught on objects including oyster leases. Further, while the drogues have reasonably small floats, moderate to high surface winds also impact their transport paths. However, in most instances, the drogues provide important information on travel times between different locations in the estuary, particularly in riverine channels where flow stratification (where the surface layer of the water moves faster than the bed) can occur on out-going tides.

Figure 4-4 GPS drifter drogues

4.6 Water level monitoring

Water level is an important metric for understanding estuarine hydrodynamics. Although real-time water level data is available from MHL for all study estuaries (see Section 2.3), in some estuaries, pilot modelling identified several important areas where additional water level data would be beneficial for model calibration. In these locations, Solinst Levelogger 5 water level sensors were deployed for the duration of each field campaign. As these instruments measure depth based on a pressure transducer, adjustments for changes in atmospheric pressure were applied based on a Solinst Barologger 5 barometric pressure sensor deployed over the same period. Once deployed, each water level sensor was surveyed using an RTK-GPS to adjust measured depth to water level elevation in AHD to be in a consistent datum with the MHL data.

In many of the study estuaries, NSW Food Authority operate water level loggers maintained by ICT International for use by the oyster farming industry. These sensors were initially deployed as part of the 2017 to 2020 Food Agility CRC project: “Oyster industry transformation – Building sustainability and profitability in the Australian Oyster Industry”. WRL surveyed these instruments using an RTK-GPS to adjust the water levels to AHD.

4.7 Conductivity and temperature profile measurements

Conductivity is used as a proxy for salinity, where the specific conductivity (which is also adjusted for the impacts of temperature) of ocean water is approximately 55,000 µS/cm. Throughout the estuaries, depth profiles were completed at targeted times of the tide. Salinity profiles were measured by lowering a Sontek EXO3 equipped with a conductivity and depth probe vertically through the water column. These profiles provide insight into whether there is density stratification throughout the water column (water increases in density throughout the water column).

5 Numerical modelling package

5.1 Preamble

Numerical modelling for each estuary in this project was completed using the RMA modelling suite (King, 2015; King, 2024), including:

- RMA-2 for two-dimensional hydrodynamic modelling
- RMA-10 for three-dimensional hydrodynamic modelling
- RMA-11 for water quality modelling
- RMA-TRK for particle tracking

A brief description of these models is provided in this section.

5.2 Two-dimensional depth averaged hydrodynamic model (RMA-2)

For the majority of the systems considered, hydrodynamic modelling was undertaken using RMA-2, a two-dimensional depth averaged finite element model that solves the shallow water equations and is suitable for simulation of flow in vertically well-mixed water bodies such as complex riverine environments. RMA-2 calculates a finite element solution of the Reynolds form of the Navier-Stokes equations for turbulent flows. The finite element method represents the fluid continuum as a series of discrete elements connected at nodes and develops a solution for the reduced system. Elements are irregularly shaped quadrilaterals and triangles of varying sizes, composing a model mesh. The use of an irregular mesh is particularly useful in allowing detail in areas of interest or rapidly varying flow, while lower resolution is used in other areas, decreasing required computational time. Furthermore, assemblages of one and two-dimensional elements may be used in the same network, leading to further computational savings. Irregular finite elements can capture irregular estuarine geometry more accurately than regular grids, avoiding problems associated with discretising a solution into a regular grid as with a finite difference model.

The main internal model parameters applied to the model are eddy viscosity and bed friction (Manning's n). RMA-2 simulates the process of bank wetting and drying, as the water level changes, through the use of marshing elements. Marshing simulates drying by approximating elements with a smaller width and higher friction for water transfer thereby effectively preventing flow in those elements while conserving mass. Marshing parameters may be varied to capture the characteristics of different intertidal terrain. The parameterisation and geometry of each model was varied to calibrate each model, the details of which is provided in the estuary specific reports.

5.3 Three-dimensional hydrodynamic model (RMA-10)

In both Port Stephens and Batemans Bay (Clyde River), the wide and open nature of the bays means that winds can combine with tides to establish currents which dominate the advective transport of plumes. Further discussion on the choice of model dimensionality is provided in Section 6.2.2. For these estuaries, hydrodynamic modelling was completed using RMA-10 which is a three-dimensional finite element model used to simulate stratified flow. The shallow water form of the Navier-Stokes equation for three dimensions together with the continuity equation are used to describe the flows. The equations are modified to make the assumption of hydrostatic pressure to facilitate the solution of the free surface problem. Momentum and continuity are both solved in the horizontal plane, but only continuity is solved in the vertical. Hence, the model cannot resolve any vertical acceleration, however this is not common in estuarine conditions. RMA-10 also has the ability to simulate density driven processes resultant from variable salinity, temperature and suspended sediment, however, this capability was not used for this project.

RMA-10 transforms horizontal triangle and quadrilateral elements into prisms, creating new nodes at either predefined depths or at sigma transforming coordinates. RMA-10 also has the capacity to include one-, two- and three-dimensional elements in the same network. Thus, RMA-10 shares with RMA-2 the advantages of a flexible finite element network, and ease of parametrization, with the added ability to simulate vertically stratified flow.

5.4 Water quality model (RMA-11)

The water quality component of this project involved modelling the propagation of conservative (non-decaying) constituents through the model domain. This was done using RMA-11, a finite element water quality model which solves for constituent concentrations using RMA-2 or RMA-10 hydrodynamic results as an input to the water quality model. The propagation of constituents in the model depends on advection (transport with net water movement, driven by hydrodynamics) and dispersion, which creates mixing and dilution. Dispersion rates are controlled by the diffusion coefficient, an input into RMA-11, and can be fixed or scaled by element size, velocity or both. RMA-11 uses an Eulerian approach to model water quality, where equations are solved at fixed locations (model mesh nodes) in space and describes how the water moves past these points in space over time.

5.5 Particle tracking model (RMA-TRK)

RMA-TRK is a Lagrangian random walk particle tracking model, also using hydrodynamic results from RMA-2 or RMA-10 as an input. The model computes advection using the hydrodynamics results and dispersion based on a provided diffusion coefficient which controls the distance a particle can randomly disperse. This was used to simulate model transport of particles which were then compared to drifter drogue velocities, and to calculate the travel time in rivers where density driven stratification can result in the top of the water column moving faster than deeper layers (see Section 7.5). Unlike RMA-11, RMA-TRK uses a Lagrangian approach, where individual particles are tracked through space and time, which can be useful to describe small scale (sub-grid) movements of particles in the model domain.

6 Hydrodynamic model development

6.1 Preamble

To predict the hydrodynamics of each estuary and to investigate the fate of sewage overflows, numerical models were developed for each of the study estuaries, based on the pilot models, data collated from existing sources and data collected during the field campaigns. The accuracy and suitability of each hydrodynamic model was verified against water level and flow data (methods outlined in this section), while the ability to represent contaminant transport in the system was verified against field campaign dye releases (refer Section 7).

This report summarises the method for the development of the models across each of the 11 estuaries in this study. Specific information about each model can be found in the estuary specific results reports (refer Table 1-2).

6.2 Mesh development

6.2.1 Bathymetry

For the majority of the modelled estuaries, high resolution digital elevation models (DEMs) were available and used for the entrance and lower reaches of each estuary (DPIE, 2018). However, the available DEMs had limited coverage in most estuaries beyond the first 1 to 2 km inland from the entrance. Further inland from the entrance, point based bathymetry was available from an array of sources (refer Table 2-1), with resolution typically reducing with distance from the estuary mouth. In important regions such as weirs and submerged breakwaters, where survey data was collected as part of the field data collection campaign, this data was incorporated into the model.

In the upper reaches of some estuaries, no bathymetric data was available. These regions tended to be substantial distances from the oyster harvest area, and any uncertainty in the model bathymetry was deemed unlikely to substantially influence the model results. Aerial imagery, boating charts and engineering judgment were required to best estimate channel depth.

While the historic bathymetric data collated for the 11 study estuaries was extensive, it is acknowledged that the available datasets in some cases are several decades old. In many estuaries, geomorphic changes over time, such as scouring or accretion at the entrances, affects tidal prisms and tidal circulation currents. To understand the magnitude and extent of geomorphic changes, bathymetric data collected during the field data collection campaign was compared against historic data. The outcomes and implications of these findings are discussed in the estuary specific fieldwork and modelling reports (refer Table 1-2).

For this project, the most recent available bathymetry data was combined, to best represent the estuaries in their present-day condition. For some estuaries, notably Nambucca River and Shoalhaven River, multiple model geometries were constructed to test the sensitivity of the results to bathymetry. These have been incorporated into the results as detailed in the estuary specific models.

6.2.2 Model dimensionality

The RMA suite of models is capable of running in one-, two- and three-dimensions. There is often a trade-off between model complexity, uncertainty and computational efficiency. One-dimensional models are simple and quick to run, however they do not resolve water movement in lateral or vertical directions. Three-dimensional models can represent transport in longitudinal, lateral and vertical directions; however, they require high quality geometry and calibration data and are computationally slow. The difference in model run time may be orders of magnitude.

The choice of model dimensionality for this project primarily involved two considerations:

1. Data availability and relevance to the study. In the upper regions of many of the study sites, bathymetric data was often sparse or unavailable, there was a significant distance to the oyster harvest area and flow is predominantly perpendicular to the riverbanks. Therefore, in these areas one-dimensional elements were used to simplify mesh geometry. These sections were modelled as trapeziums with top width as river width, side slope and depth chosen to best match the flow area at mid tide, calculated from survey data cross sections. Conversely, in the lower reaches of the estuaries (typically near oyster harvest areas) where complex geometry typically leads to substantial lateral variance in flow and velocity, higher resolution 2D or 3D model meshes were utilised.
2. Capacity for wind driven transport as a major driver of plume transport. For most systems modelled in this project where currents are dominated by tidal currents and catchment inflows, a two-dimensional depth averaged model was used. This is because the computational efficiency of the two-dimensional model largely outweighs the shortcomings of failing to predict three-dimensional processes. For locations where large, exposed bays result in wind driven circulation influencing surface currents (e.g. Port Stephens and Batemans Bay in the Clyde River), a three-dimensional modelling approach was adopted. Note that RMA-10 is capable of running discrete areas in 1D, 2D and 3D, so only the exposed areas with sufficient depths were run in 3D. However, wind transport is modelled across the broader model domain.

As the majority of the modelling in the key areas of interest was completely in 2D, it is important to recognise that there are some implications of the assumptions inherent to depth averaged modelling. Major considerations include:

- Depth averaged models do not capture initial surface plume mixing and dispersion prior to a constituent becoming vertically well-mixed. This means that the level of dilution near the discharge point of the overflow will be overestimated. However, as the level of dilution required to reduce the risk of pathogen transport is high (six orders of magnitude), which is not reached in the immediate vicinity of a discharge location, this is unlikely to impact the usability of the results for the models intended purpose.
- Depth averaged models do not capture velocity distributions through the water column.
- Depth averaged models do not include density differences to capture the behaviour of a buoyant plume or salinity/temperature stratification. Note that the 3D models run on this project also did not include density.

The final two factors have a particular impact on the time of travel in riverine systems where stratification of flow is observed on an ebb tide more significantly than a flood tide, which is discussed further in Section 7.5.

6.2.3 Resolution

Unlike grid based hydrodynamic models, RMA allows for a mesh of irregular triangular and trapezoidal elements of varying size. As computational load is proportional to mesh size, the ability to alter resolution over the model domain allows for reduced model run times. Additionally, this feature allows for increased resolution and model stability around important features, while allowing for reduced resolution in lower priority areas and locations where limited data is available.

An irregular mesh was used in each estuary to capture important geometric features. The resolution of the model varies significantly throughout the model domain, to balance the need to capture geomorphic features which drive plume transport in the key areas of interest, maintaining model stability and computational efficiency. Higher resolution (typically elements of less than 10,000 m^2) was typically used in the lower estuary, adjacent to harvest areas, and nearby to the modelled sewage overflow simulation locations. In these areas, velocity distributions across channels have the potential to impact plume transport and the management of the oyster harvest areas. Higher model resolution was also used to improve model stability, typically either due to rapid changes in velocities (such as lagoon entrances and weirs) or near the sewage overflow locations where rapid changes in concentrations occur in the water quality model. In areas away from the areas of interest, much lower resolution was used, with elements of up to 2 km^2 in some cases.

For estuaries where a three-dimensional finite element model was used (Clyde and Port Stephens), the three-dimensional area was modelled with two layers, an upper layer 1 m deep and a second layer extending to the bed, with layer depths scaled according to the sigma transformation. This was found to be sufficient vertical resolution to capture vertical stratification caused by wind (hence simulate wind driven surface plume transport) while minimizing computational requirements.

6.3 Boundary conditions

To accurately capture system inflows and tidal hydrodynamics for model calibration and verification runs, model boundary conditions were based on timeseries data acquired during historic data collation and the field collection campaign. Inflow data at the upstream extent of the model was based on scaled catchment inflows as per Section 2.4, while ocean tidal boundaries were derived from MHL tidal data (refer Section 2.3). The nearest available offshore gauge was used as the ocean boundary in each model, with further detail on the stations used provided in the model specific reports.

For scenario modelling purposes, inflows were based on representative catchment inflows based on exceedance probabilities of observed flow. The tidal boundary scenarios were based on representative spring and neap tides from the tide level timeseries. Further details on environmental conditions are presented in Section 8.2.2.

6.4 Hydrodynamic calibration and verification

It is important for a hydrodynamic model to be able to replicate water levels, velocities, and flow throughout the model domain. This drives the advective transport within each system, which is vital to understanding the movement of a sewage overflow event around the lower estuary. To ensure that the hydrodynamic models utilised in the scenario modelling were fit for purpose and representative of the study estuary systems, an iterative process of model validation was employed. This typically involved at least two periods of comparison with field data:

1. **MHL tidal gauging periods (from 1986 to 2010)**
   Based on the available historic bathymetric data, a mesh for each system was created and run using boundary conditions corresponding to the period of the MHL tidal flow gauging studies (refer Section 2.3). Model parameters, including the model mesh (bathymetry, geometry, and resolution) and friction parameters were refined to ensure the model was capable of sufficiently replicating observed tidal water levels and flows (typically to within 10% of observed flow in the areas of interest). In some estuaries, multiple historic gauging programs were available. In these cases, multiple periods were run and compared to gauged data, to ensure the model had satisfactory performance in all periods. In systems with mobile bathymetry, this could also be used to test sensitivity to bathymetry, which is discussed in estuary specific reports. Periods for model calibration varied between estuaries based on data availability and is discussed in each report.

2. **2023 Field data collection**
   During each field data collection campaign, additional hydrodynamic data was collected to verify the model. Model meshes were updated to reflect any updated bathymetry collected. The model was subsequently run for the period of field data collection and compared to the collected data and model parameterisation was refined. In some estuaries, notably Nambucca and Shoalhaven Rivers, several model bathymetries were required in scenario runs to account for highly mobile shoals and entrances which were found to have a significant impact on results. Further information can be found in the relevant estuary reports.

Determining whether a model is sufficiently calibrated to be fit for purpose involves use of engineering judgment. The decision of when an individual model was fit for the purpose of simulating sewage transport to oyster harvest areas was made via consultation between the primary modeller and other engineers with modelling expertise. This decision focused on whether the hydrodynamics of the model were sufficiently well matched to the measured data to ensure confidence that the model would accurately represent transport within the areas of interest (near overflow locations and harvest areas), to an appropriate level of confidence considering other sources of uncertainty in the model. In general, this involved achieving a good fit of the tidal prisms, peak discharges and shapes of the tidal discharge curves, using reasonable model parameters. If a good fit was unable to be achieved at any location, consideration was given to whether this would impact model results, and where relevant, sensitivity analysis was undertaken. The specifics determining how each model was deemed fit for purpose is discussed further in the estuary specific reports.

For estuaries where sufficient data was available to fully calibrate the model using preexisting data, the 2023 WRL fieldwork data was used as separate (blind) verification or validation data. The process of verification ensures the model is not overfit to the calibration period and is able to represent the estuarine processes adequately in other periods. The process of verification involved the comparison of the 2023 hydrodynamic data to the model results using the previously calibrated parameters, with the same bathymetry as for calibration, or only minor changes in bathymetry to reflect the 2023 data. In some estuaries, either where large bathymetric changes occurred between the hydrodynamic data sets, or preexisting hydrodynamic data was too sparse, there was insufficient data to have separate verification data, and all datasets were used for calibration. In these cases, geometry and parameters were closely inspected to ensure they were reasonable and representative, and the increased uncertainty created by the lack of verification was considered in sensitivity analysis and reporting of the results. This is discussed in the estuary specific reports.

6.5 Parameters

6.5.1 Hydrodynamic coefficients

All models used a scaled turbulent exchange (eddy viscosity) coefficient of 0.5. This coefficient was scaled by element turbulence length scale computed from the dimensions of the element (such that a larger element will have higher turbulence than a smaller element) via the methods described in King (2024). In some isolated areas of high velocities and turbulence, such as a culvert, a higher eddy viscosity was used to capture the turbulence and increase model stability.

Models had varying Manning's n (roughness) coefficients, generally in the range of 0.015 to 0.035 in sandy channels and greater values in intertidal areas. Roughness coefficients used are specified in estuary specific reports.

6.5.2 Timestep and model output

All hydrodynamic models used a timestep of 0.2 hours or 12 minutes. Results were output at every model timestep (12 minutes).

6.6 Limitations for future model use

The models created for this project have been constructed and calibrated to an extent to be fit for the purpose of modelling transport from overflow locations to harvest areas. The models may be appropriate for other uses, however, the limitations must be considered. Specific limitations are discussed in the estuary specific reports, however there are some general considerations that apply to all models, including:

- Models have more refinement, higher resolution, and better calibration in the areas of interest (generally the lower estuary). Model accuracy may be reduced in other areas.
- Models may have reduced accuracy into the future if bathymetric changes occur. Moreover, for estuaries which experience regular bathymetric changes (Nambucca River, Wallis Lake, Shoalhaven River and Clyde River) sensitivity of model results to bathymetry was considered and appropriate changes were made. These conclusions may not apply for other model use cases.
- Neither the two- or three-dimensional models explicitly simulate any density driven processes.
- Vertical velocity differences are not simulated in the two-dimensional depth average models.
- Though the three-dimensional models do simulate differing vertical velocities, these models were constructed only to predict the general circulation patterns likely to be driven by wind from different directions, and were not calibrated, nor do they have sufficient vertical resolution, to accurately predict the full velocity distribution created by wind shear, or vertical mixing processes.
- Catchment inflows have been included simplistically in these models, by scaling inflows from the nearest WaterNSW flow gauge. In some instances, these gauges do not cover substantial areas of the catchment upstream of the tidal limit. While this was considered appropriate for this use, this may not be the case for other uses.

7 Water quality model development

7.1 Preamble

In water quality modelling, there are two main processes which move constituents within a water body:

- Advection, net movement with the current
- Dispersion, which is mixing which causes the constituent to spread out over time

In RMA-11, the first of these two processes is modelled using direct outputs from the hydrodynamic model (RMA-2 or RMA-10). Shear based mixing at scales larger than the mesh resolution was explicitly modelled using the hydrodynamic results, however sub-model scale dispersion was modelled using a bulk diffusion coefficient parameter, which was refined using the field data collection.

The following section provides a discussion on dispersion and modelling pollutant transport in RMA-11, including:

- An introduction to dispersion (Section 7.2)
- An overview of the method for deriving model dispersion coefficients from dispersion theory and field data (Section 7.3)
- A discussion on the method and limitations of plume dispersion modelling in RMA-11 (Section 7.4)

7.2 Theoretical dispersion

Mixing or dispersion in estuaries is driven by turbulence and shear (variation in velocities between adjacent currents). While more complex, high resolution models are able to resolve more of the circulations, eddies and shear in a system, some processes occur below the resolution of the model. Models (including RMA-11) simulate such sub-mesh scale dispersion through diffusion, the random scattering of particles. The diffusion equation for Fickian 2D diffusion is:

$$\boldsymbol{C(x,y,t) = \frac{M}{d4\pi Dt} e^{-\frac{x^2+y^2}{4Dt}}} \qquad \textbf{Equation 1}$$

Where:
$C_{(x,y,t)}$ is the concentration at point (x, y) and time t
M is the concentration of the constituent at the boundary (in kg)
x and y is the distance from the initial location (in m)
t is the time since diffusion commenced (in seconds)
d is the representative depth (assumed to be 1 m in calculations) (in m)
D is the diffusion coefficient (in m^2/s)

This equation accounts for physical mixing processes in an estuary through the diffusion coefficient (D) which is selected appropriate for the resolution of the model and the amount of dispersion occurring in the system the model is representing. These coefficients are not based on physical constants and must be obtained from empirical methods or laboratory experiments. The hydrodynamic models used in this project are high resolution and resolve some dispersion (or mixing) explicitly. Dispersion that is explicitly resolved includes:

- Lateral shear across the channel
- Circulations above mesh scale

Three-dimensional models also resolve vertical shear, however two-dimensional depth averaged models do not.

Mixing that is not included explicitly in the models of this study include:

- Sub mesh scale turbulence
- Density driven mixing (which was not included in the models of this study)

These dispersion processes not resolved explicitly in the model are represented by the diffusion coefficient. For the water quality modelling used for each estuary, RMA-11 diffusion coefficients were determined from data obtained during the Rhodamine dye release experiments, and model simulations of these releases (see Section 4.4).

One-dimensional regions of the model domain do not resolve lateral dispersion explicitly, and most mixing must be captured by the diffusion coefficient. However, these sections are usually located in the upstream reaches of the model, not near harvest areas.

7.3 Field derived dispersion values

As discussed in Section 4.4, dye experiments were completed in 10 estuaries (no fieldwork was completed on the Tweed River) to inform the parameterisation of the water quality model. Across the 10 estuaries, 37 dye releases were conducted in the lower reaches of each estuary, including five in slow moving bays or lakes and the remainder in tidal channels.

To obtain estimates of plume spreading dispersion rates for each estuary, the decrease in peak concentration from the dye release experiments over time was analysed. In this analysis, movement of the peak (advection) was not considered. During each dye release, transects were taken across the plume to capture the plume width and peak concentration at a point in time (refer Figure 7-1). From the set of all transects, a subset of representative peak concentrations was compared to theoretical estimates of maximum plume concentrations over time (calculated using Equation 1), as shown in the example for Wallis Lakes in Figure 7-2. The combined plume dispersion result for all estuaries is shown in Figure 7-3. Most dye experiments involved releasing 500 mL of dye, however in some cases a smaller or larger volume was released. To allow them to be readily compared, concentrations were scaled to match an initial release volume of 500 mL before plotting.

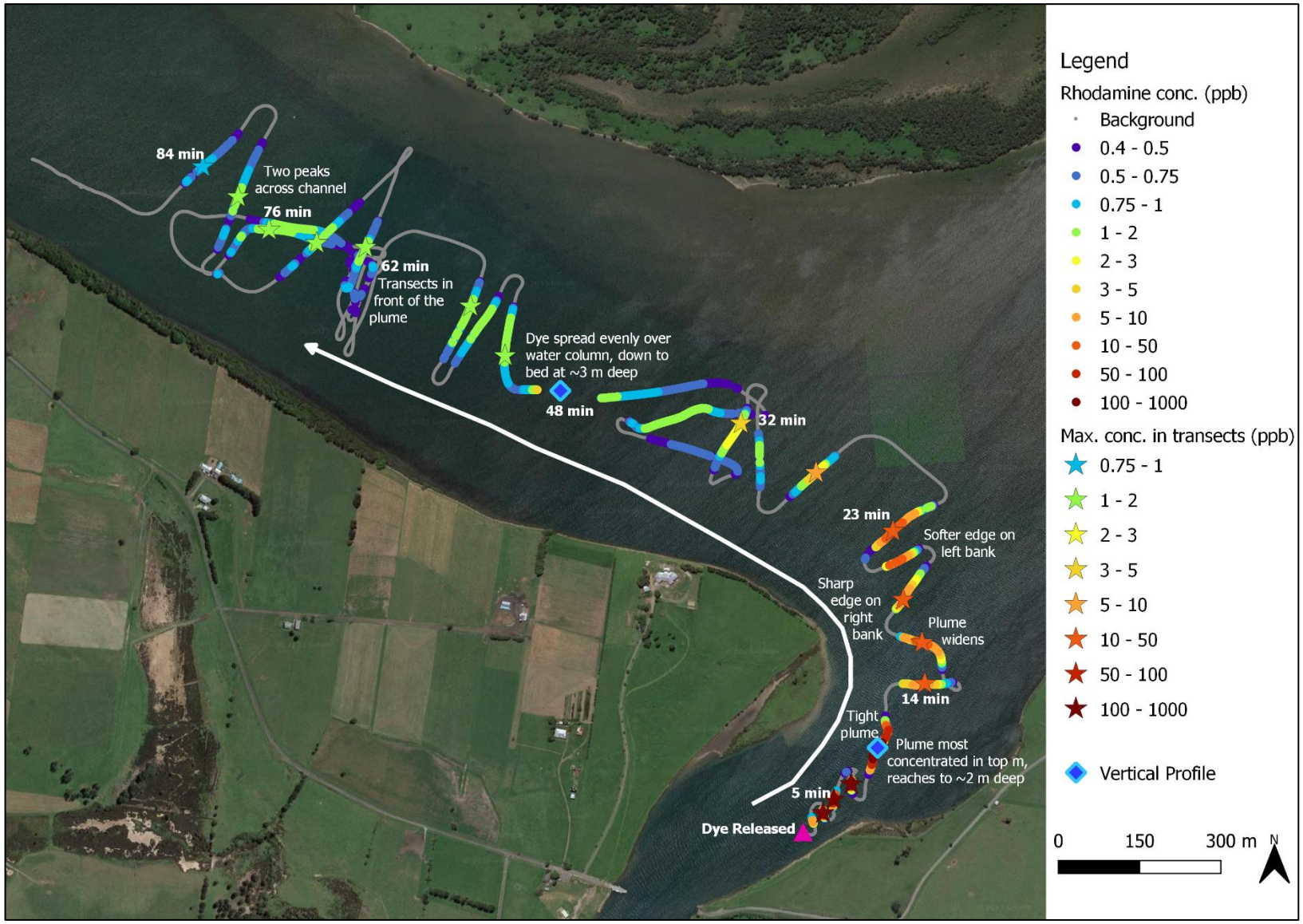

Figure 7-1 Dye release on the Shoalhaven River demonstrating plume transect crossings

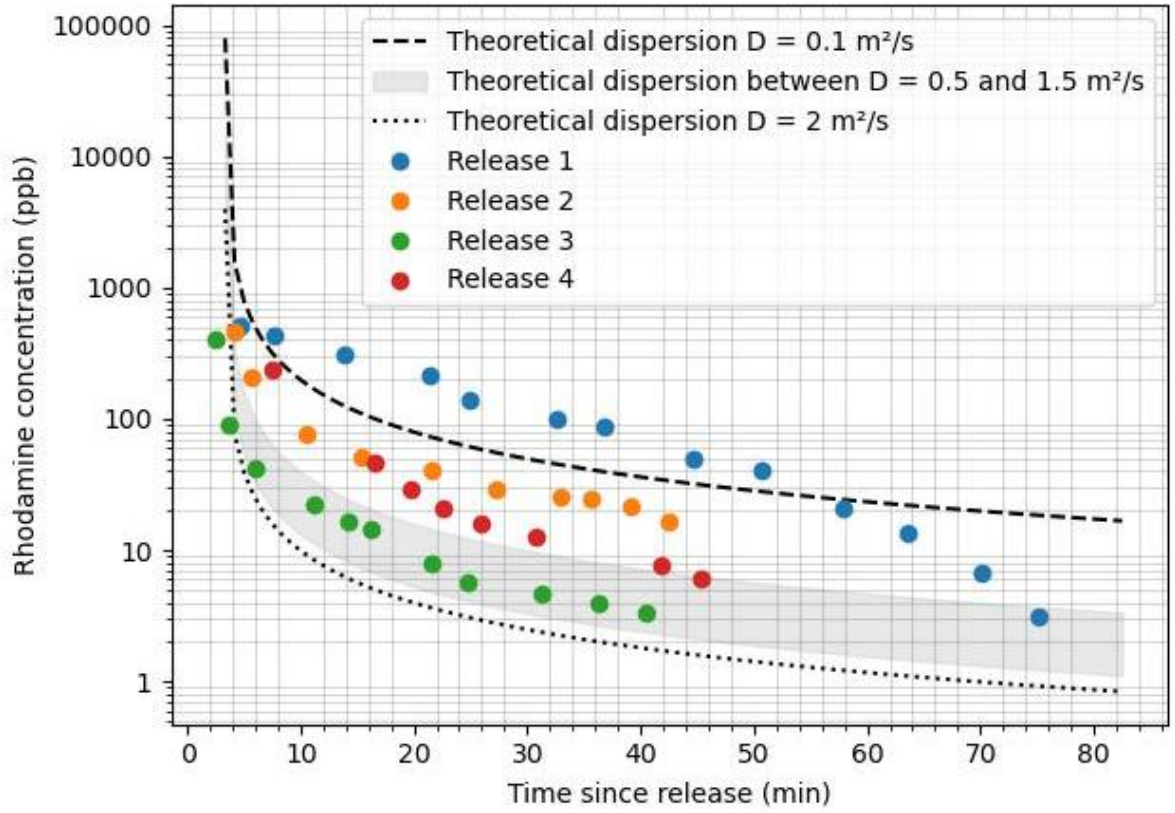

Figure 7-2 Maximum concentrations from select transects from four dye releases conducted on Wallis Lake, compared to theoretical 2D diffusion values

When comparing the observed peak observations to theoretical dispersion, most field dispersion values fall within a range of D = 0.1 and 2 m^2/s, with the most common range 0.5 to 1.5 m^2/s. There is, however, considerable scatter and substantial variation between releases, both within individual estuaries and between different estuaries. Site specific drivers of outlier values and uncertainty are discussed in individual estuary reports (see Table 1-2), however, there are a number of general factors which contribute to the large dispersion range observed. These factors include:

- The accuracy of the fluorometer decreases at higher concentrations, and values over 100 ppb are less reliable.
- This approach assumes the measurements are taken at the peak of the plume. In reality, transects are unlikely to have gone through the exact peak of the plume, thus many are likely underestimates of the peak concentration.
- The theoretical dispersion calculations assume two-dimensional dispersion. Vertical profiles conducted during fieldwork show that the plume initially spreads in three dimensions (vertically and laterally), before becoming vertically well mixed over time. Prior to full vertical mixing, the field measurements (which are concentrations at a single depth near the surface) are greater than the two-dimensional theoretical dispersion estimates. However, this usually only affects the first 15 minutes (especially for faster moving releases), and fitting was primarily done based on data from after this point.
- Dispersion is related to depth and velocity (Elder, 1959). Higher velocities and greater depths lead to greater dispersion. This can explain much of the variability in dispersion observed. However, this analysis did not quantitatively consider the relationship between these variables and dispersion.

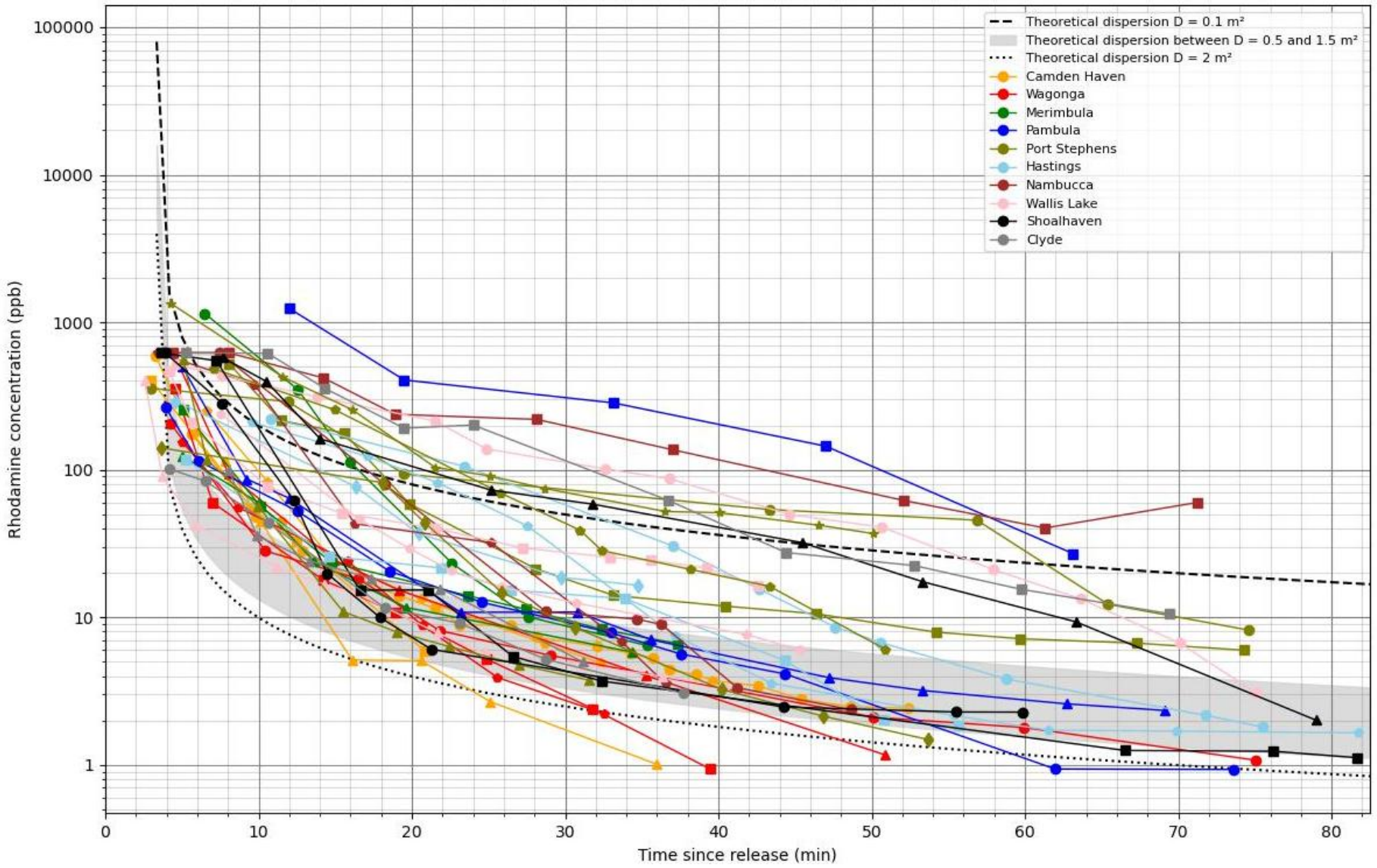

Figure 7-3 Observed and theoretical plume dispersion behaviour for all study estuaries

In the 10 study estuaries, similar trends were observed: dispersion rates were related to velocity, with releases in fast-moving channels having higher dispersion rates than releases in lakes and releases at the peak of the tide having higher dispersion rates than at the change of the tide. This is because these releases were subject to higher shear and turbulent mixing, causing greater plume dispersion. The theoretical approach (Equation 1) models all of this dispersion through a constant diffusion coefficient, regardless of turbulence and velocity. However, RMA-11 resolves some of this variability in dispersion explicitly via the hydrodynamic models. Therefore, theoretical dispersion calculations will give higher diffusion coefficients than those necessary in RMA to match the dispersion behaviour of dye plumes.

While the field data provides valuable data in determining appropriate diffusion coefficients to an order of magnitude, it is acknowledged that there is still uncertainty in a specific rate of dispersion appropriate for modelling. This uncertainty and the impact of model results is discussed below in Section 7.4.

7.4 Modelling dispersion in RMA-11

7.4.1 Dye release dispersion verification

Theoretical field derived dispersion rates (refer Section 7.3) were used to determine reasonable upper and lower diffusion coefficient ranges. These coefficient ranges were verified in RMA-11 by simulating the field dye release experiments (refer Section 4.4).

Dye releases were modelled by setting the starting concentration of a conservative constituent in the element closest to the dye release location to match the highest recorded dye concentration. While this approach creates some initial numerical instability, due to sharp concentration gradients, and is sensitive to the initial size of the element to which mass is added (which was sized to match the early plume), it is representative of the rapid dye release which occurred during the field experiments. It was found that a refined mesh, with small element sizes near the dye release location, was needed to simulate the steep concentration gradients near the dye release location without excessive numerical instability.

The modelled results were compared against measured dye concentrations and observations made by WRL staff during the field experiments. General considerations regarding model dispersion verification against field derived coefficient values include:

- The concentration and size of the first cell has a large impact on modelled plume behaviour. As fluorimeter accuracy is reduced for high concentrations outside of the instrument calibration range (refer Section 4.4), there is a high degree of uncertainty associated with the initial observed peak concentration. As a key model input, variations in this initial concentration will impact the total mass of pollutant in the model and dispersion behaviour.
- For hydrodynamics run using RMA-2, the model simulates two-dimensional dispersion only, while the field measurements are observing three-dimensional dispersion which transitions to two-dimensional if the plume becomes vertically well mixed. Consequently, the model is likely to overestimate concentrations as the initial mass assumes vertical mixing over the entire water column.
- For hydrodynamics run using RMA-2, due to velocity stratification, model plume advection may be underestimated. Consequently, modelled peak concentration and plume width may become spatially offset from observed results. This offset increases with time since initial release. Section 7.5 discusses how this has been managed in the results.

Twenty-seven dye release experiments were simulated in RMA-11, with similar findings. An example of model verification of dye release experiments on the Camden Haven estuary is shown in Figure 7-4. It was found that, as would be expected, using a smaller diffusion coefficient results in a narrower, more concentrated plume, while a larger coefficient results in a plume that spreads further and faster. In general, diffusion coefficients in the range of 0.5 to 1.5 m^2/s satisfactory replicated plume behaviour, however it was found that in some instances, the modelled plume travelled slower than was observed in the field, due to velocity stratification, especially in cases of tidal straining, as discussed in Section 7.5. It was found that a fixed model diffusion coefficient (rather than one scaled by velocity or element size) provided the best replication of dye release experiments. This is likely due to the fact that dye releases occurred over a limited space and period of time, hence model velocities and element sizes did not vary greatly within releases.

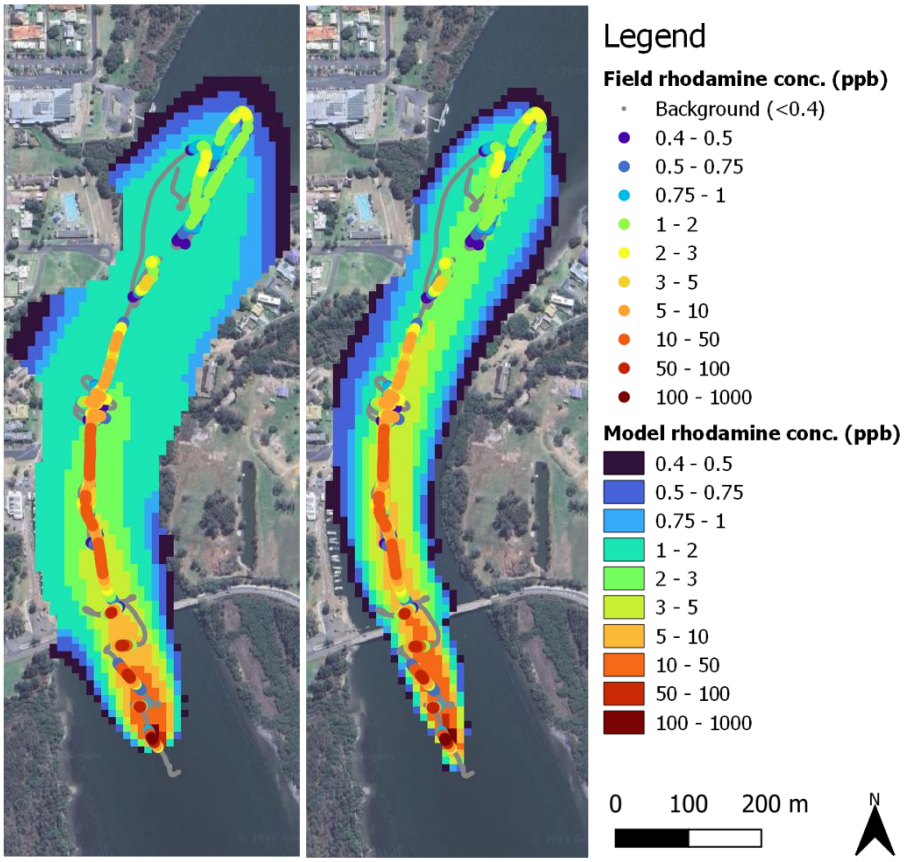

Figure 7-4 Model verification of Camden Haven dye release 2, with background colour showing model results and overlaid points showing field measurements. Maximum value at each point during the entire period of the simulation using D = 1.5 m2/s (left) and D = 0.5 m2/s (right)

A Lagrangian method for simulating the dye release experiments, using the RMA-TRK particle tracking model was also trailed. This method was able to simulate plume spread, and further validated the appropriateness of the 0.5 to 1.5 m^2/s range for diffusion coefficients. However, a Lagrangian method was not pursued for scenario runs due to difficulties in interpreting results in a meaningful way for the intended purpose of these models (as concentration is not explicitly modelled).

Model simulation of dye releases verified the appropriateness of the theoretically derived upper and lower diffusion coefficient bounds, the use of depth averaged models (in cases where velocity stratification is minimal) and revealed the need to have a highly refined mesh near dye release or overflow locations. Given the high degree of uncertainty in calculating dispersion values and issues associated with dye release modelling, it was determined that modelling of the dye release plumes could not further refine the choice of dispersion coefficients in the model (beyond the range identified in Section 7.2), and further sensitivity testing was completed which is discussed in Section 7.4.5.

7.4.2 Simulation of overflows in RMA-11

To simulate a sewage spill, conservative (non-decaying) constituents, simulating a pollutant, were added to the model at relevant locations. For water quality scenario runs, all model boundaries (except those related to the overflow locations) were set to a constant constituent concentration of zero (e.g. no pollutant inflows from these boundaries). All constituents that reach the tidal boundary are removed from the system. The model boundaries all extend into the ocean to account for this.

As these constituents are conservative, unless the constituent reaches the downstream boundary of the model (the ocean), the total mass of contaminant is conserved across the model domain, although the plume is transported and the peak concentration reduced via the processes of advection and diffusion. The implications of this are discussed further in Section 8.4.

Although it is recognised that dispersion is related to velocity (as discussed in Section 7.3 and established in Elder (1959)) this project used fixed diffusion coefficients (not scaled by velocity). This was chosen both because fixed coefficients gave better results when replicating dye release experiments, and because the aim of the use of upper and lower diffusion coefficients was to bound the expected ranges of dispersion, rather than replicate expected dispersion. Thus, by using a fixed coefficient, there was certainty on what diffusion was applied in the model, and hence certainty that the range required was being simulated.

7.4.3 Timestep and model output

A timestep of 0.05 hours or 3 minutes, was used in RMA-11 models, with smaller timesteps during and immediately after the overflow to increase model stability. Hydrodynamic input results (at a 12 minute timestep) were interpolated linearly to obtain the smaller timestep for the RMA-11 model. RMA-11 results were output at timesteps ranging from 30 mins to 3 minutes, depending on the temporal resolution necessary to capture the movement of the plume adequately (i.e., a smaller timestep is required to show the movement of a plume appropriately in a very fast moving system when compared to a slow one). The results output is detailed in the estuary specific reports.

7.4.4 Mesh refinements

As was found during the simulation of dye release experiments, additional numerical dispersion and erroneous mass generation (or loss) may occur due to poorly formed mesh, insufficient mesh resolution, and large run timesteps. Following the development of the hydrodynamic models as outlined in Section 6, model mesh geometries were tested in RMA-11 for numerical stability and mass conservation. Meshes were refined where necessary, and both the hydrodynamics and water quality models re-run.

7.4.5 Diffusion coefficient sensitivity testing

To test the implications of uncertainty surrounding diffusion coefficient selection, detailed sensitivity analysis was run for a single estuary (the Shoalhaven) on short duration dry weather spills. The primary purpose of this investigation was to assess the sensitivity of diffusion coefficient choice and any implications for oyster harvest area operational decision-making criteria (plume dilution and travel time). The diffusion coefficients used for sensitivity testing were 0.5 and 1.5 m^2/s, based on the ranges from comparison with theoretical dispersion rates (see Section 7.2).

In general, scenarios with a higher diffusion coefficient will lead to greater dilution and plume spreading, leading to the plume reaching more areas, though at a lower concentration. Figure 7-5 and Figure 7-6 show this behaviour. These figures show the minimum dilution (i.e., maximum concentration) observed at each point during the entire scenario period, rather than the results at any single timestep. In the higher diffusion scenario, the plume spreads laterally enough to reach Comerong Bay. Meanwhile, in the lower diffusion scenario, the plume does not reach Comerong Bay. However, changes in diffusion coefficient can also have much more complex impacts, in situations where diffusion may impact whether a plume reaches a junction before the change of a tide or other such instances. For example, as can be seen in Figure 7-7 and Figure 7-8, showing a spill on mid ebb tide from Orient Point, with a higher diffusion coefficient, the plume disperses into the main channel and most of the plume leaves the model domain before the tide turns. However, with a lower diffusion coefficient, the plume does not fully disperse out of the shallow area near the overflow location before the tide turns, pushing the plume upstream, thus it reaches the harvest areas in the Crookhaven River at a high concentration.

These examples have been chosen to demonstrate the potential differences between runs with different diffusion coefficients. However, for the majority of scenarios, resulting concentrations observed in harvest areas were generally consistent to an order of magnitude of dilution and tidal cycle resolution (6 hour) travel time between scenarios run with a diffusion coefficient of 0.5 and 1.5 m^2/s. Nevertheless, to deal with the uncertainty in appropriate dispersion coefficients, all scenario modelling permutations (refer Section 8.2.3) were run using a range of diffusion coefficients derived from the field data (0.5 to 1.5 m^2/s) to capture cases where subtle changes may significantly impact plume dilution and travel time to harvest areas. The results presented for the scenario testing are the maximum concentration observed at each point in either of the two model runs ($D = 0.5$ and $D = 1.5$ m^2/s), and the travel times presented are the minimum time for the plume to reach each harvest area (at 5,000,000 times dilution) in either of the two model runs.

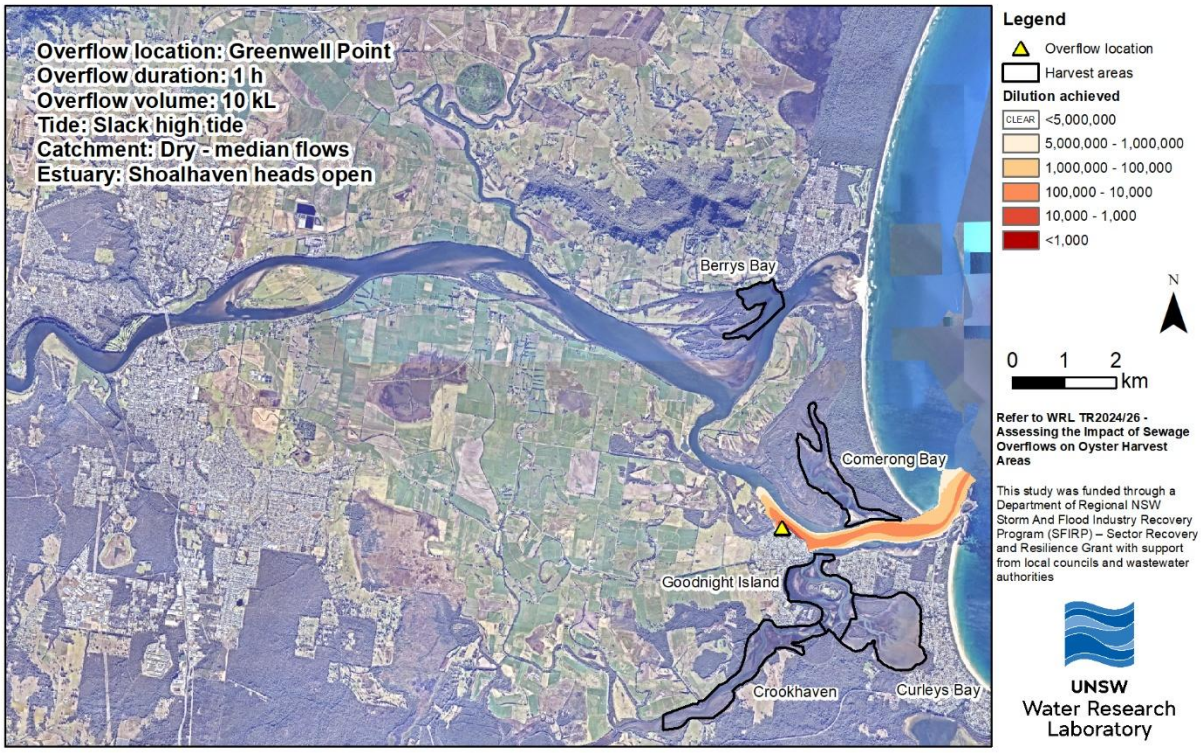

Figure 7-5 Modelled spill from Greenwell Point on a slack high tide with D = 0.5 m^2/s*

*Result figures present the minimum dilution (i.e., maximum concentration) observed at each point during the entire scenario period (21 days).

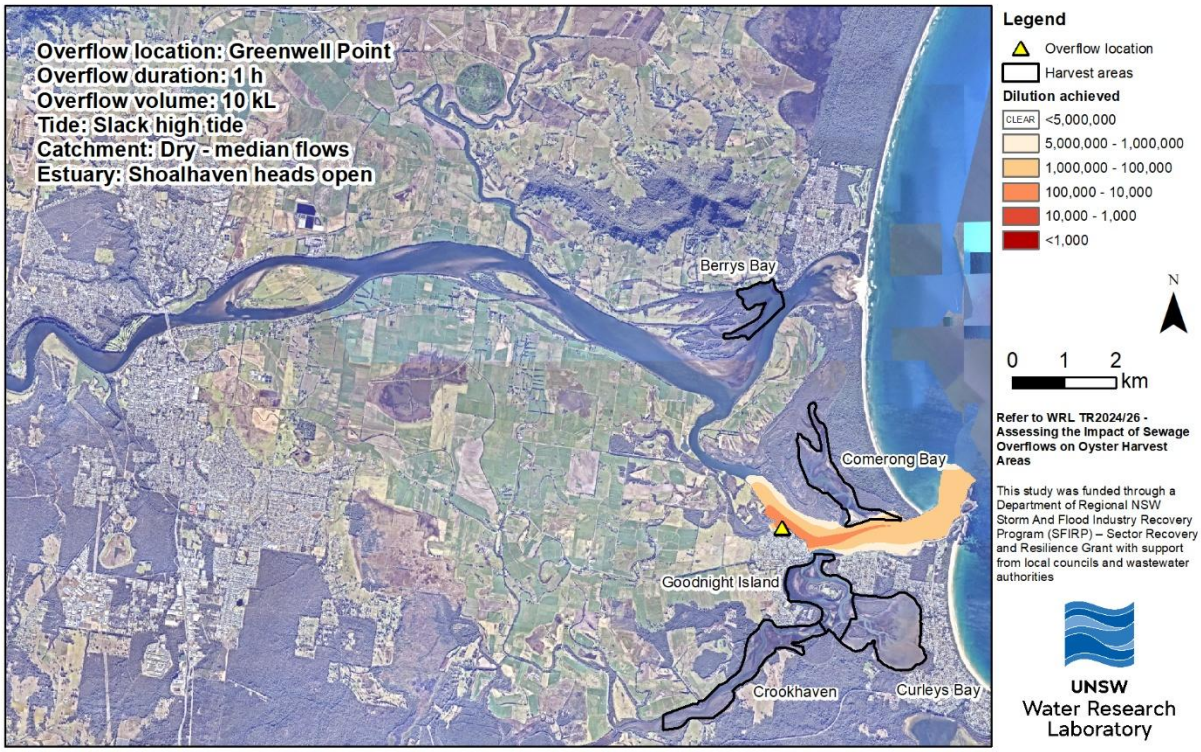

Figure 7-6 Modelled spill from Greenwell Point on a slack high tide with D = 1.5 m^2/s*

*Result figures present the minimum dilution (i.e., maximum concentration) observed at each point during the entire scenario period (21 days).

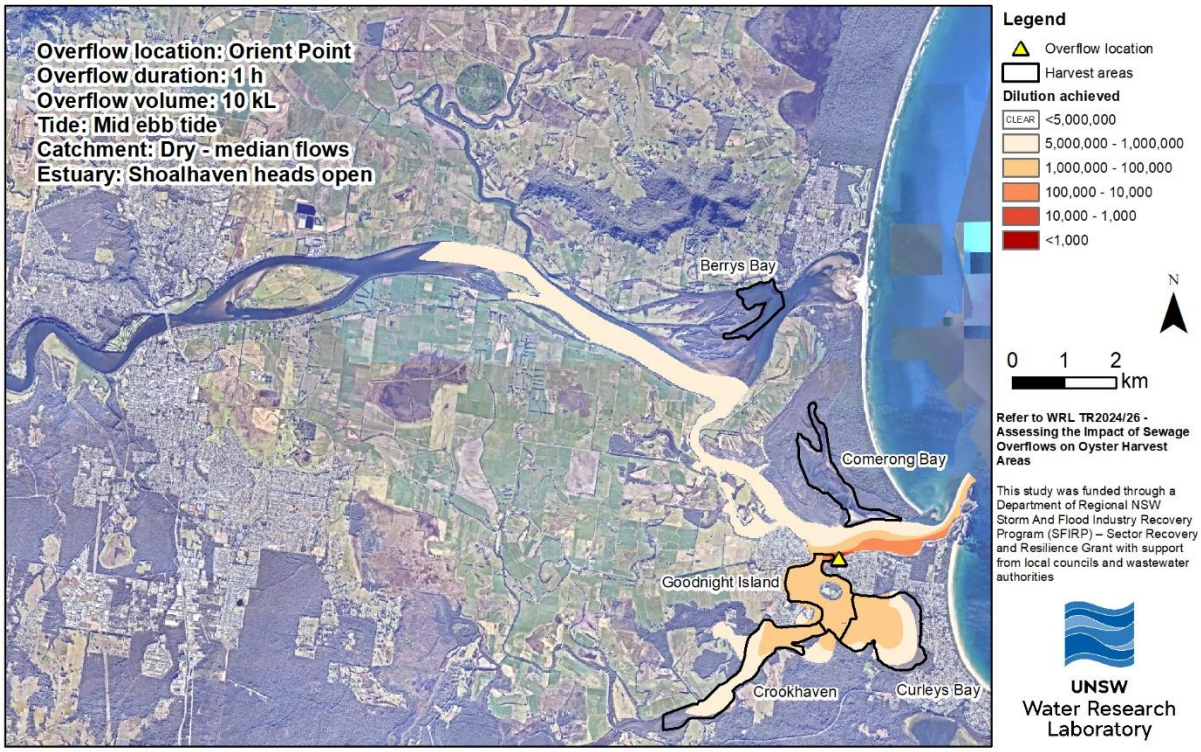

Figure 7-7 Modelled spill from Orient Point on a mid-ebb tide with D = 0.5 m^2/s*

*Result figures present the minimum dilution (i.e., maximum concentration) observed at each point during the entire scenario period (21 days).

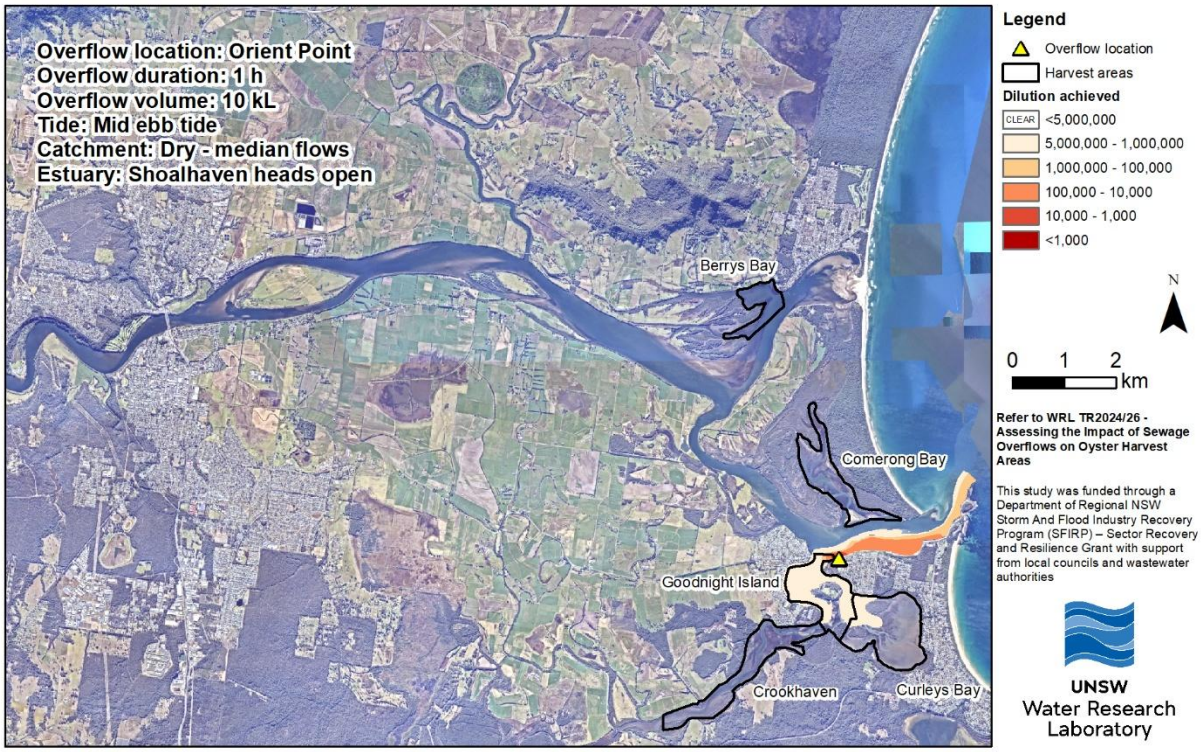

Figure 7-8 Modelled spill from Orient Point on a mid-ebb tide with D = 1.5 m^2/s*

*Result figures present the minimum dilution (i.e., maximum concentration) observed at each point during the entire scenario period (21 days).

7.5 Tidal straining

In many estuaries, a velocity distribution exists through the water column. Typically, higher velocities are observed at the surface and lower velocities near the bed, due to the friction. A two dimensional, depth averaged model uses a single velocity to represent the whole water column, as seen in Figure 7-9.

In many cases, the vertical velocity distribution is symmetrical between the ebb and flood tide. Tidal straining is a specific case of density driven flow, whereby the distribution is asymmetrical between tides. On an ebb tide, buoyant fresh water flows faster over denser saline water, creating larger velocity distribution (Simpson et al., 1990). On the flood tide, as denser, saline water enters the estuary the density profile is less and 'stands up', resulting in much less vertical velocity distribution. These dynamics can be seen in Figure 7-9 and Figure 7-10. This effect is seen in areas where there is a significant saline gradient which moves up and down the estuary (i.e., in riverine estuaries, in the transition zone between fresh and saline), and is not simulated in the depth averaged model.

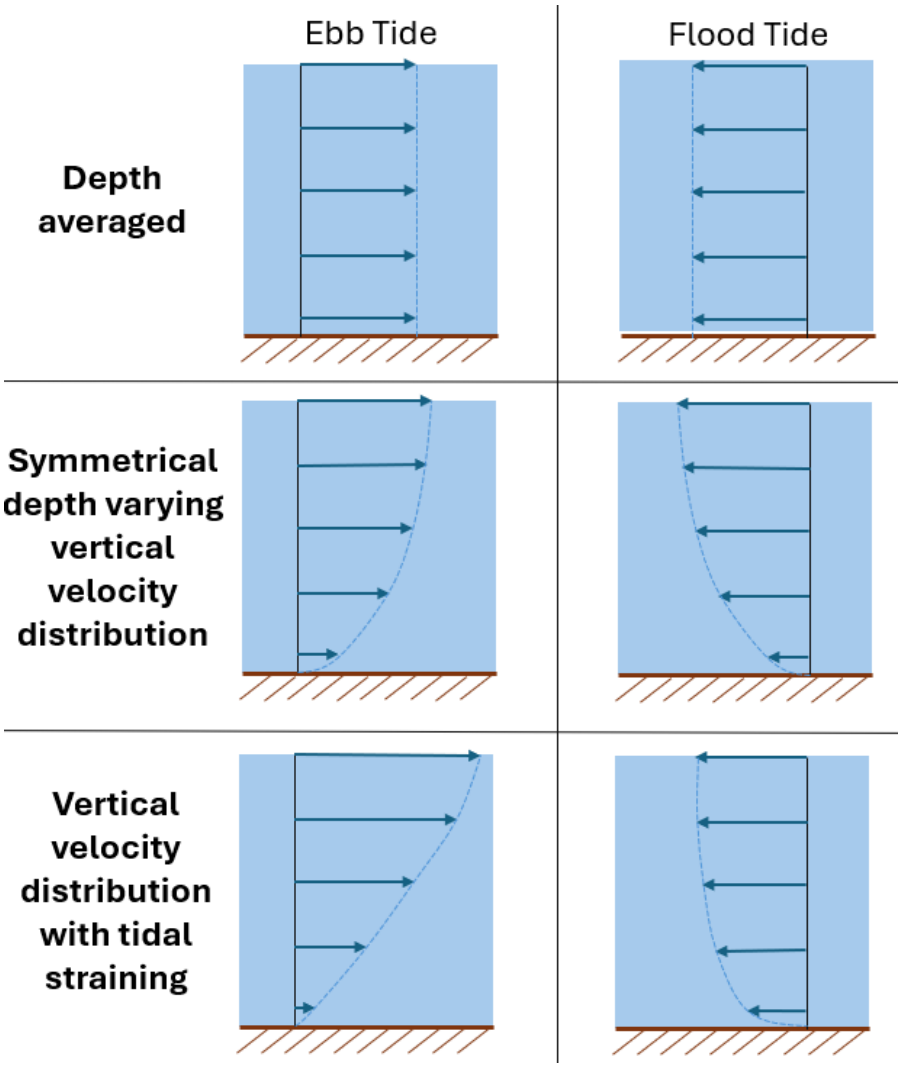

Figure 7-9 Vertical velocity profiles for depth averaged flow, flow with tidally symmetrical depth varying velocity profiles and tidal straining with non-symmetrical velocity profiles

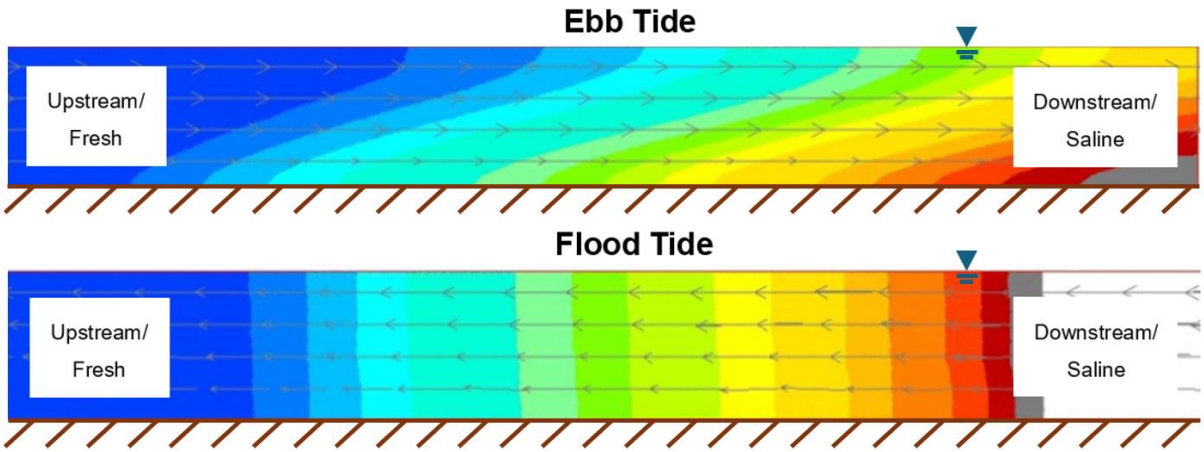

Figure 7-10 Schematic of tidal straining. Red colours represent more saline water and blue colours represent fresher water.

To quantify the effect of vertical velocity distribution, travel times of GPS drifter drogues (see Section 4.5), which travel with currents near the surface, were compared to the travel times of particles released from the same location in the depth averaged model, using RMA-TRK, the particle tracking module of RMA (see Section 5.5). Since a vertical velocity distribution causes the surface to move faster than the average of the water column, when comparing GPS drogue data to modelled particles, the GPS drogues usually moved faster, with the difference being greatest on the ebb tide (see Table 7-1 and Figure 7-11 for examples). To compensate for the potentially faster surface currents conveying pollutants faster than predicted by depth averaged currents, a velocity scaling factor was determined, which resulted in modelled particles matching drogue movements observed in the field, as can be seen in Figure 7-11.

Table 7-1 Ratios of drogue travel time measured in the field to modelled particles on the Nambucca River for ebb and flood tides

Drogue drop	Tide	Ratio (observed distance travelled over modelled distance)
Day 1 drop 1	Ebb	1.88
Day 1 drop 2	Flood	1.15
Day 2 drop 1	Ebb	2.10
Day 2 drop 2	Ebb	1.74
Day 2 drop 3	Flood	1.10
Day 3 drop 1	Ebb	1.85

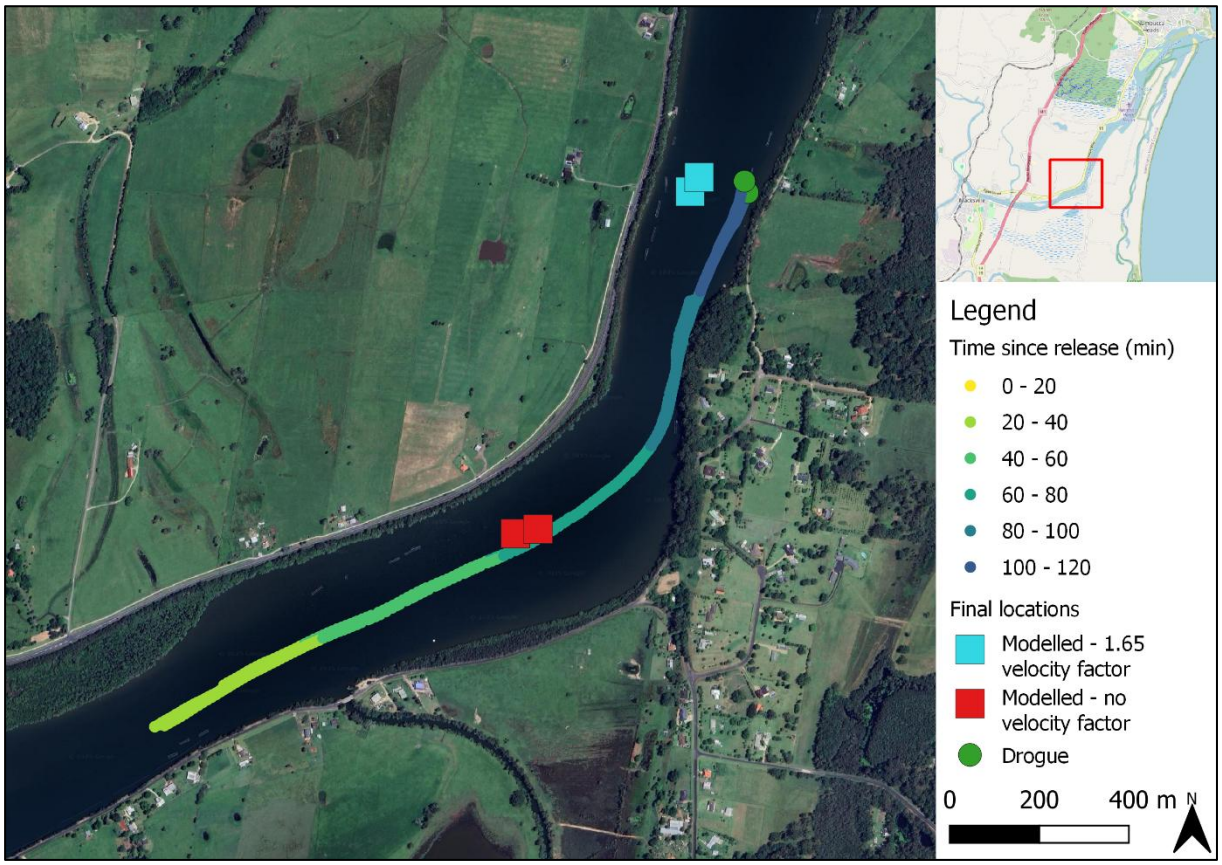

Figure 7-11 Example of drifter drogue model simulation using a velocity factor vs field data on ebb tide on the Nambucca River

In some estuaries, observed drogue to model ratios were near one (meaning the system approximates depth averaged flow). In others depth varying vertical velocity distributions were observed (ratios significantly greater than one), however these distributions were tidally symmetrical (similar ratios on the ebb and flood tides). Finally, in some estuaries, tidal straining was observed (asymmetrical vertical velocity distributions, where ratios were much bigger on the ebb tide than on the flood tide). In these cases, asymmetry was also visible in ADCP transects (see Figure 7-12).

In cases where a depth varying vertical velocity distribution is present, movement of the portion of the plume in the upper portion of the water column would be faster than is simulated in a depth averaged model. However, in cases where this distribution is symmetrical between tides, net plume transport over multiple tides would remain the same, as faster transport would be counteracted by equivalent velocity distributions on the opposite tide. Reported travel times are banded by 6 hour (tidal cycle) increments (as discussed in Section 8.3.3), so over this period, a vertical velocity distribution is unlikely to have an effect on the reported timing of plume arrival. Hence, despite observed vertical velocity distributions which resulted in faster transport at the surface, no timing adjustments were applied to systems where distributions were symmetrical between tides.

In estuaries where tidal straining (asymmetrical vertical velocity distributions) was observed, this would have an effect on net plume transport over multiple tidal cycles. Tidal straining would have the effect of longitudinally spreading out the plume, as upper parts of the water column travel faster and lower parts travel slower on the ebb tide, and this is not fully counteracted by the flood tide stratification. The centre of mass of the plume, provided it is vertically well mixed before ebb tide, would travel at a similar rate with or without tidal straining. Thus, the concentration results of the model were deemed suitable for the overflow locations affected by tidal straining. However, as the front edge of the plume would be stretched out, arriving downstream faster (at a more dilute concentration) the speed of plume travel in the model was not considered representative of the real world.

Tidal straining effects were observed in drogue releases and flow transects (see Figure 7-12) on the Nambucca, Hastings and Shoalhaven Rivers, and is considered to potentially impact the upstream release locations on these estuaries:

- Bowraville and Macksville WWTPs (Nambucca River)
- Wauchope WWTP (Hastings River)
- Berry and Bomaderry WWTPs (Shoalhaven River).

In these cases, plume timing was corrected for by the methods described in Section 8.3.4.

The effects of tidal straining in these estuaries could be more accurately simulated using a three-dimensional model. However, it was determined that depth averaged (two-dimensional) modelling along with timing adjustments provided suitable information, whilst minimising model computational time, hence allowing for a greater number of model scenarios to be simulated.

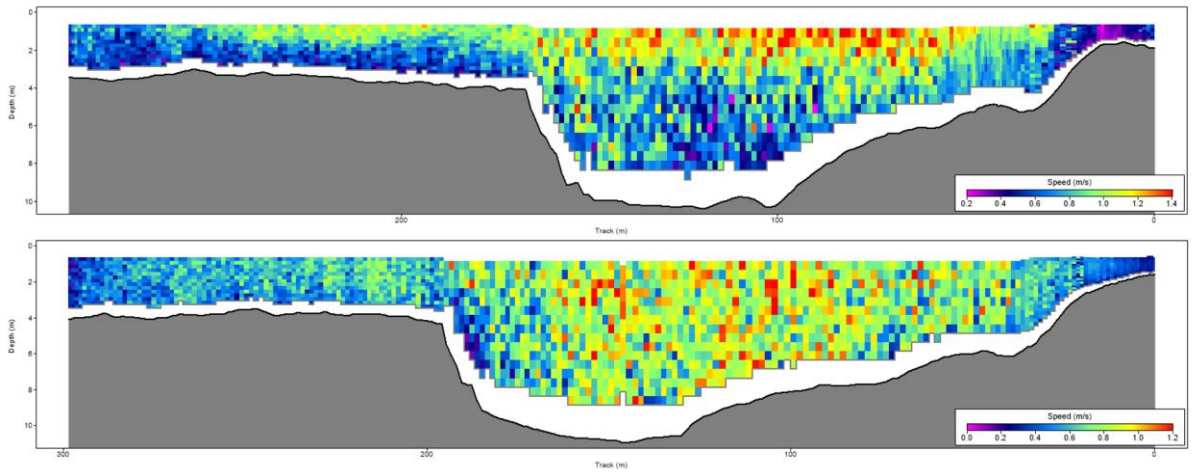

Figure 7-12 ADCP flow transects at the same location on the Hastings River showing velocity stratification on the ebb tide (upper) and no stratification on the flood tide (lower)

8 Scenario modelling

8.1 Preamble

The advantage of modelling is that a large range of hypothetical scenarios can be run, reflecting conditions that may occur in the future. Models were set up to ensure that a wide range of scenarios, which approximate many potential conditions could be simulated, rather than simulating a small range of conditions to a much higher degree of certainty. Scenarios were carefully chosen to ensure that they would capture a broad range of potential conditions that might be experienced. Despite the range of model scenarios completed, it is likely no real event will exactly match any particular run. Users of the results are encouraged to use these as a tool to guide decision making following overflows, rather than as a prediction of exact concentrations during any given event.

For each estuary, the range of possible overflow and environmental conditions were considered and the various combinations of these conditions were run as individual scenarios. This section details the various conditions considered, and the processing of results.

8.2 Scenario variables

For each estuary an array of model scenarios were included, each with a different set of overflow and environmental conditions, to characterise the spectrum of overflow events that might be expected. The conditions modelled are summarised in Table 8-1.

Table 8-1 Suite of overflow and environmental conditions used for constructing model scenarios

Condition	Conditions modelled
Location	Estuary specific
Duration/Volume	1 h – 10 kL
	3 h – 30 kL
	10 h – 100 kL
	30 h – 300 kL (Port Stephens only)
	100 h – 1000 kL (Port Stephens only)
Tide	Slack high tide
	Slack low tide
	Mid ebb tide
	Mid flood tide
Catchment condition	Dry – median flows
	Wet – 80th percentile flows
	Wet – 95th percentile flows

Condition	Conditions modelled
Estuary entrance condition (Nambucca River and Shoalhaven River)	Estuary specific
Wind direction (Port Stephens and Clyde River)	None North (5 m/s) North east (5 m/s) East (5 m/s) South (5 m/s) West (5 m/s)

8.2.1 Overflow conditions

For each estuary, between three and seven overflow locations were chosen, based on historical overflow data and discussions with NSW Food Authority. Though the simulated overflow locations were limited, they were chosen to be representative of all overflow possibilities. For the purposes of modelling, all overflows were modelled with a nominal initial concentration of 1,000 mg/L, which was used to calculate the level of dilution achieved.

All overflows were simulated at a rate of 10 kL/h (i.e., a 3 hour long spill would be 30 kL). For all estuaries, 10, 30 and 100 kL spills were simulated, with additional 300 and 1000 kL spills simulated for Port Stephens, due to its large size.

8.2.2 Environmental conditions

For each estuary, a suite of environmental conditions considered relevant to the estuary were modelled, including consideration of:

- **Stage of the tide**
  For all estuaries, overflows occurring at four points of the tide were simulated. This allows for assessment and prediction of whether overflows are influenced by incoming and outgoing tides. As tidal peaks occur at different times and at different points in the estuary, simulation conditions are referenced to MHL water level gauging points, with details and lag times specified in model results and individual estuary reports.

- **Size of the tide**
  For some estuaries, the size of the tide an overflow occurred on (i.e., whether the tide had a large or small tidal range) was found to be significant for model results. For these estuaries, scenarios occurring on different sizes of the tide were modelled, with details presented in individual reports.

- **Catchment inflows**
  Catchment inflows were represented as constant flows at the upstream boundaries of the model. Different catchment conditions were modelled as flowrates representing percentiles of long term scaled WaterNSW flow gauging (as described in Section 2.4). The higher the flow percentile, the wetter the conditions (e.g. the 80th percentile flow is greater than the observed flow 80% of the time).

- **Estuary entrance condition**
  Estuary condition was considered relevant for estuaries with untrained morphodynamic entrances, hence experiencing large bathymetric variability, such as Nambucca and Shoalhaven (Shoalhaven Heads). Merimbula also has a variable untrained entrance, however it was established that the entrance state did not functionally effect scenario outcomes for this use case. For these two estuaries, multiple mesh geometries, with different bathymetries, were simulated, as discussed further in the estuary specific results.

- **Wind**
  Wind was run as a variable for the two large bay systems, Port Stephens and Clyde, which were modelled in three dimensions. For these estuaries, scenarios simulated a constant wind of 5 m/s from the four cardinal directions, as well as northeast (as this is a common wind direction detected at nearby weather stations), for the entire simulation period. A constant wind of 5 m/s for a 21 day period is unrealistic but these scenarios provide predictions of the range of transport that might arise. Judgment is required in interpreting scenarios simulating wind, and the results from two or more different scenarios may need to be consulted to consider the limits of possible situations.

For some estuaries, some environmental conditions (such as catchment inflows) were found to have an insignificant impact on results after preliminary runs were completed. In these cases, the full suite of scenarios for this variable was not run. Details of which environmental variables were run for each estuary, and whether a full suite of iterations was completed for each variable are detailed in the estuary specific reports.

8.2.3 Sensitivity analysis

To account for uncertainty in some parameters, multiple model variations were run for a single reported scenario. For all scenarios, the model was run twice, with two diffusion coefficients (0.5 and 1.5 m^2/s) to account for uncertainty in the dispersion, as discussed in Section 7.4.5. The results presented are the minimum dilution (i.e., highest concentration) experienced at each point in either of the two model runs (for both the figures and the values for dilution in each harvest area). The timings are the minimum time for the plume to reach each harvest area (at 5,000,000 times dilution) for either of the two model runs, including consideration of tidal straining (see Section 7.5).

Some estuaries had other model variations run to account for model sensitivity, that were then combined into a single scenario via the process described above. These variations accounted for sensitivity to model parameters or bathymetry. This is discussed in further detail in the relevant estuary specific report.

8.3 Reported results

8.3.1 HTML tool

The results of all modelled scenarios have been compiled into a user-friendly HTML tool, presenting scenario results in tabular form, with links to figures of results. A description of the tool, and further interpretation of the results are described in the overview report (WRL TR2024/26).

8.3.2 Dilution

Dilution at any location and time is the concentration at that location and time divided by the starting concentration. For example, if an overflow occurred at 1000 mg/L, and reached a harvest area at 0.001 mg/L, the dilution achieved is 1,000,000 times. The higher the dilution achieved, the lower the concentration when it reaches the harvest area. Results have been presented as dilutions (rather than absolute concentrations) based on feedback from NSW Food Authority.

8.3.3 Timing

Arrival times for plumes were extracted for each model run as the time taken (from the start of the overflow) for the plume to reach the harvest area at 5,000,000 times dilution. Travel times have been grouped into bands of <6 hours, 6-12 hours, 12-24 hours, and daily increments beyond 24 hours, as there is insufficient certainty in travel times to report sub tidal cycle differences. For overflows where tidal straining (see Section 7.5) was considered an issue, the timing of the plume was adjusted based on this analysis instead of the raw RMA11 model data.

8.3.4 Timing corrections for cases involving tidal straining

As discussed in Section 7.5, upstream overflow locations on the Hastings, Nambucca and Shoalhaven Rivers were considered affected by tidal straining, which would affect the arrival time of plumes. To calculate appropriate arrival times in cases of tidal straining, particle tracking (RMA TRK) was used. Simulated particles were tracked at regular intervals along the river to determine the distance travelled in one tide (ebb and flood) for a king tide. Then a velocity factor of two was applied to every ebb tide travel distance and the number of tidal cycles required for a particle to reach the harvest areas from the upstream overflow locations was calculated. The velocity factor of two was chosen as it was a representative maximum of the velocity factors observed when comparing drogue releases to modelled particles based on observed data on the three relevant estuaries (refer Section 7.5). This process was repeated for different catchment inflow conditions and estuary conditions.

This process accounts for the faster transport of the front edge of the plume in the three identified systems due to tidal straining, but will in most instances still predict a faster travel time than expected in reality, for a variety of reasons, including:

- The chosen velocity factor of two is larger than the average velocity factor observed.
- The reach where tidal straining is considered to be occurring in this method is large (to the tidal extent). In reality, tidal straining would occur to varying degrees along this stretch depending on the salinity gradient and may not occur in upper reaches of the Nambucca and Broughton Creek.
- The tide chosen to simulate transport distances is the largest tide in a year. The average tide would transport particles significantly less distance.

However, as this information may be used to make decisions regarding consumer safety, this provides a conservative estimate of travel time for the purpose of decision making.

8.3.5 Interpreting model results

This project has pre-emptively simulated a series of overflow scenarios to aid in rapid decision making when sewage overflows occur, in order to avoid the time consuming process of running models to simulate real overflow events when they occur. Actual overflow situations are unlikely to exactly match a simulated scenario, and some interpretation or interpolation between results may be necessary. For overflows of different volumes or concentrations, this can be done quantitatively from the results provided. For example, a 1 kL spill over 1 hour will be analogous to a 10 kL spill over 1 hour except that the severity is reduced by an order of magnitude (i.e., if the modelled dilution at a harvest area is 10,000 times in the 10 kL spill would be 100,000 times diluted from the 1 kL spill).

Note that the duration of release may be relevant in certain scenarios. For example, a 1 hour overflow on a mid-ebb tide may entirely leave the estuary before the turn of the tide, but a 3 hour overflow starting at the same time may not. Care should be taken to match the duration as closely as possible, as well as the volume. As duration only impacts the direction of transport for spills over less than a single tidal cycle, for long duration spills (>10 hours), the 10 hour results should be used, and can be scaled to any observed volume of the overflow.

For other variables, such as timing, or catchment inflow, an overflow is unlikely to perfectly match any scenario run. In these cases, the two (or more) model scenarios that the situation overflow falls between should be considered. The difference between these two model scenarios and the real-world overflow can be subjectively interpolated to determine the outcome for the specific overflow situation. However, if there is uncertainty about the outcome, the worst case of the two or more relevant model scenarios being considered should be used. Similarly, if one or more variables about the spill, for example timing or duration, are not known, the suite of modelled scenarios relevant to the known variables should be considered, and the worst case scenario of possible outcomes should be used, until more information becomes available.

8.3.6 Grouping

In many cases, scenarios with varying environmental conditions resulted in very similar results of minimum dilution and minimum travel time. To simplify viewing of the results, scenarios with functionally similar results were grouped into one table entry. This provides users of the results with more concise information which is aimed at improving ease of interpretation. To group the results, the minimum (e.g. worst case) dilution and timing is presented in the final results. This typically only occurred when the order of magnitude of dilution in each harvest area and timing of plume arrival was consistent across all oyster harvest areas in the estuary. In some cases, this was also utilised where it was assessed as unlikely that decision makers would have sufficient information to distinguish between results (e.g. the bathymetric conditions near the entrances of Nambucca River).

In general, the criteria for grouping was that the dilution for all harvest areas falls in the same dilution band (>5,000,000 or did not reach, 5,000,000 to 1,000,000, 1,000,000 to 100,000, 100,000 to 10,000 and 10,000 to <1,000) and that time of plume arrival falls in the same or adjacent band (<6h, 6 to 12 h, 12 to 24 h, 24 to 48 h, 2 to 3 d, etc.). These rules are general and in some cases, similar runs were grouped when results were very similar, but dilutions fell on either side of a band, and some runs were not grouped when plume transport was substantially different despite results falling in the same bands.

Expert judgement was used in these cases. Less importance was placed on dilutions matching bands for very high concentrations (<100,000 times dilution). In some cases, runs with different results were grouped due to modelling uncertainty. These cases are discussed in the estuary specific reports. Stage of the tide was grouped for all 10 h (100 kL) scenarios. It is acknowledged that some uses of the modelled data may require further detailed information. Individual scenario runs making up a grouped run are still accessible to users. An example of grouping is shown in Table 8-2 and Table 8-3. Table 8-2 shows a group in Camden Haven estuary where scenarios for different catchment conditions are combined. By clicking on ‘view sub-runs’, in the rightmost column, the constituent runs can be seen, as in Table 8-3.

Table 8-2 Example run grouped by catchment condition for Camden Haven estuary

Catchment condition	Tide	Overflow duration	Overflow volume	Hanleys Point		Stingray Creek		Gogleys Lagoon		04_Camden_Haven	View sub-runs
				Dilution	Time	Dilution	Time	Dilution	Time		
All	Slack low tide	3 h	30 kL	250,000	<6h	7,900	<6h	460,000	<6h	View Figure	View

Table 8-3 Constituent sub runs for example run grouped by catchment condition for Camden Haven estuary

Discharge location	Combined ID	Catchment condition	Tide	Overflow duration	Overflow volume	Hanleys Point		Stingray Creek		Gogleys Lagoon		04_Camden_Haven
						Dilution	Time	Dilution	Time	Dilution	Time	
North Haven	00_CAM_WQ_1_3h	Wet - 80th %ile flows	Slack low tide	3 h	30 kL	280,000	<6h	8,000	<6h	530,000	<6h	View Figure
North Haven	00_CAM_WQ_1_3h	Wet - 95th %ile flows	Slack low tide	3 h	30 kL	250,000	<6h	7,900	<6h	460,000	<6h	View Figure
North Haven	00_CAM_WQ_1_3h	Dry - median flows	Slack low tide	3 h	30 kL	280,000	<6h	8,000	<6h	540,000	<6h	View Figure

8.4 Impact of decay

As discussed in Section 7.4.1, the model uses a conservative (non-decaying) constituent to simulate sewage pollution. While decay of viruses in surface water systems is known to occur, there is significant variability in the decay rates for relevant viruses in scientific literature. Of particular interest for this study is human noroviruses and hepatitis A, which have some of the most scarce information on decay in literature (Boehm et al., 2019).

Based on the systematic review of seven mammalian virus decay rates, Boehm et al. (2019) found that noroviruses were typically the most persistent in water bodies (i.e., decay the slowest) and therefore the remainder of this section focusses on these viruses species. Boehm et al. (2019) showed the median decay rate value, k, for noroviruses from the available literature was 0.08 d^{-1} (8% per day). with a range of 0.006 to 0.37 d^{-1}. It is noted that all the data available was for experiments in freshwater, and all bar one value was done in the dark. Both saltwater and sunlight are expected to increase virus decay. A more recent study, Desdouits et al. (2022) completed experiments measuring genomic concentrations of noroviruses in seawater, and showed that at least two strains of norovirus can remain infectious for several weeks in seawater as well. Their experiments suggest a median decay rate of 0.16 d^{-1} (16% per day) with a range between 0.03 to 0.20 d^{-1}. Based on the available information, there is significant variance in potential decay rates of the relevant viruses, between <1% and 37% decay per day (<0.01 d^{-1} and 0.37 d^{-1}). This range introduces considerable additional uncertainty if decay rates are included in the model.

Sensitivity tests were completed on the model to understand the impact of inclusion of decay. As scenarios with long travel times were needed to observe the impact of decay, Port Stephens (a large estuary) and Wagonga (an estuary with a large lake in which transport is slow) were selected to test decay. Scenarios for a 10 hour, 100 kL overflow during median catchment inflow conditions (with no wind for Port Stephens) were run without decay and with decay of 0.15 d^{-1}. Results for locations reached within 48 hours were largely unchanged, and decay only substantially reduced concentrations in harvest areas reached after several days.

These scenarios (large estuaries with large spills that may still be at high concentrations after multiple days) were chosen as they are some of the only situations in which harvest areas that are reached after a relatively long travel time. In most cases, harvest areas are reached within less than 48 hours. Thus, decay would not substantially affect the interpretation of the majority of model runs. Furthermore, considering the level of uncertainty in the decay rates and the human health implications of overestimating decay, inclusion of decay in the model was not considered suitable. However, in cases where the plume takes a substantially long time (several days or more) to reach the harvest areas, decay may reduce the risk of contamination to oysters.

8.5 Use of results

The results of these models should be interpreted with user discretion. They are intended as a tool to be used in the decision making process, rather than an indication of the exact prediction of dilutions which will result in different areas. Discretion should be used, especially in cases where:

- The overflow and environmental conditions are in between or outside of simulated conditions (especially wind conditions)
- The edge of a transported overflow is near a harvest area, even if not quite inside it
- Decay might be a significant consideration (for locations where it takes longer for sewage to reach)
- Other estuary specific cases referred to in the individual estuary reports.

9 Conclusion

This report is one of two overview reports produced for the study “Assessing the impact of sewage overflows on oyster harvest areas in NSW”. The purpose of this report is to provide technical managers with a summary of the methods of data collation, fieldwork data collection and numerical modelling utilised for all estuaries in this study. Key information included in the report relates to the integration of existing data sources, the field data collection campaign, model development, model verification, scenario modelling and modelling limitations.

This report, along with the project overview report (WRL TR2024/26), support each of the 11 estuary specific field and modelling reports (refer Table 1-2). This report is intended to be read in conjunction with individual technical reports developed for each estuary (refer Table 1-2). Results of the scenario modelling is available in the accompanying tool, which is documented in the overview report WRL TR2024/26.

10 References

AHO 2024a. AusENC Coastal Pack CST04 - Gladstone to Port Macquarie. Australian Hydrographic Office.

AHO 2024b. AusENC Coastal Pack CST05 - Port Macquarie to Eden. Australian Hydrographic Office.

Boehm, A. B., Silverman, A. I., Schriewer, A. & Goodwin, K. 2019. Systematic review and meta-analysis of decay rates of waterborne mammalian viruses and coliphages in surface waters. *Water research,* 164**,** 114898.

Desdouits, M., Polo, D., Le Mennec, C., Strubbia, S., Zeng, X. L., Ettayebi, K., Atmar, R. L., Estes, M. K. & Le Guyader, F. S. 2022. Use of Human Intestinal Enteroids to Evaluate Persistence of Infectious Human Norovirus in Seawater. *Emerg Infect Dis,* 28**,** 1475-1479.

DPIE 2018. NSW Marine LiDAR Topo-Bathy 2018 Geotif. Department of Planning, Industry and the Environment.

Elder, J. W. 1959. The Dispersion of a Marked Fluid in Turbulent Shear Flow. *Journal of Fluid Mechanics,* 5**,** 544-560.

Gallant, J., Wilson, N., Dowling, T., Read, A. & Inskeep, C. 2011. SRTM-derived 1 Second Digital Elevation Models Version 1.0. *In:* AUSTRALIA, G. (ed.).

King, I. 2015. Documentation RMA-11 – A Three Dimensional Finite Element Model for Water Quality in Estuaries and Streams 4.4C, Resource Modelling Associates, Sydney Australia.

King, I. P. 2024. Documentation - RMA2 - A TWO DIMENSIONAL FINITE ELEMENT MODEL FOR FLOW IN ESTUARIES AND STREAMS Version 9.0H.

NAVONICS. 2023. *NAVONICS Chart Viewer SonarChart* [Online]. Available: https://webapp.navionics.com/ [Accessed 2023].

NearMap. 2024. *NearMap MapBrowser* [Online]. Available: https://apps.nearmap.com/maps/ [Accessed 2024].

OEH. 2022a. *NSW Office of Environment and Heritage (OEH) Multi-beam Bathymetry Surveys* [Online]. Available: https://catalogue-imos.aodn.org.au/geonetwork/srv/eng/catalog.search#/metadata/60160b01-8ffc-45ce-a6f4-ee70ce391ec6 [Accessed 2022].

OEH. 2022b. *NSW Office of Environment and Heritage (OEH) Single-beam Bathymetry and Coastal Topography Surveys* [Online]. Available: https://catalogue-imos.aodn.org.au/geonetwork/srv/eng/catalog.search#/metadata/8b2ddb75-2f29-4552-af6c-eac9b02156a6 [Accessed 2022].

Simpson, J. H., Brown, J., Matthews, J. & Allen, G. 1990. Tidal Straining, Density Currents, and Stirring in the Control of Estuarine Stratification. *Estuaries,* 13**,** 125-132.

WaterNSW. 2023. *Continuous water monitoring network* [Online]. Available: https://realtimedata.waternsw.com.au/water.stm [Accessed 2023].